

**RECONSTRUCTING EXTINCT PLANT WATER USE FOR UNDERSTANDING
VEGETATION–CLIMATE FEEDBACKS: METHODS, SYNTHESIS, AND A CASE
STUDY USING THE PALEOZOIC-ERA MEDULLOSAN SEED FERNS**

JONATHAN P. WILSON,^{1*} JOSEPH D. WHITE,² WILLIAM A. DIMICHELE,³ MICHAEL T. HREN,⁴
CHRISTOPHER J. POULSEN,⁵ JENNIFER C. MCELWAIN,⁶ and ISABEL P. MONTAÑEZ,^{7*}

¹Department of Biology, Haverford College, 370 Lancaster Ave., Haverford, PA 19041 USA
<jwilson@haverford.edu>

²Department of Biology, Baylor University, One Bear Place #97388, Waco, TX 76798-7388 USA

³Department of Paleobiology, National Museum of Natural History, Smithsonian Institution,
P.O. Box 37012, Washington D.C., 20013-7012 USA

⁴Center for Integrative Geosciences, University of Connecticut, Beach Hall 207, U-1045,
354 Mansfield Road, Storrs, CT, 06269 USA

⁵Department of Earth and Environmental Sciences, University of Michigan, 2534 C.C. Little Building,
1100 North University Ave., Ann Arbor, MI, 48109-1005 USA

⁶Earth Institute, School of Biology and Environmental Science, University College Dublin,
Stillorgan Road, Belfield, Dublin 4, Ireland

⁷Department of Earth and Planetary Sciences, University of California, Davis, One Shields Avenue,
Davis, CA 95616 USA
<ipmontanez@ucdavis.edu>

*Corresponding authors

ABSTRACT.—Vegetation affects feedbacks in Earth’s hydrologic system, but is constrained by physiological adaptations. In extant ecosystems, the mechanisms controlling plant water use can be measured experimentally; for extinct plants in the recent geological past, water use can be inferred from nearest living relatives, assuming minimal evolutionary change. In deep time, where no close living relatives exist, fossil material provides the only information for inferring plant water use. However, mechanistic models for extinct plant water use must be built on first principles and tested on extant plants. Plants serve as a conduit for water movement from the soil to the atmosphere, constrained by tissue-level construction and gross architecture. No single feature, such as stomata or veins, encompasses enough of the complexity underpinning water-use physiology to serve as the basis of a model of functional water use in all (or perhaps any) extinct plants. Rather, a “functional whole plant” model must be used. To understand the interplay between plant and atmosphere, water use in relation to environmental conditions is investigated in an extinct plant, the seed fern *Medullosa* (Division Pteridospermatophyta), by reviewing methods for reconstructing physiological variables such as leaf and stem hydraulic capacity, photosynthetic rate, transpiration rate, stomatal conductance, and albedo. Medullosans had the potential for extremely high photosynthetic and assimilation rates, water transport, stomatal conductance, and transpiration—rates comparable to later angiosperms. When these high growth and gas exchange rates of medullosans are combined with the unique atmospheric gas composition of the late Paleozoic atmosphere, complex vegetation–environmental feedbacks are expected despite their basal phylogenetic position relative to post-Paleozoic seed plants.

INTRODUCTION

Land plants are the dominant biological interface affecting water flux between the soil and atmosphere. Through a series of physiological processes operating on key environmental molecules—water, carbon dioxide, and molecular oxygen—plants mediate the flux rates of these molecules within the biosphere by their responses to variations in relative humidity, insolation, and atmospheric pressure. Because plants link water, carbon, and oxygen cycles on a global scale, they also influence climate by regulating terrestrial energy budgets at short (water vapor) and long time scales (carbon dioxide and oxygen). Accurate reconstruction of past climate states through various forms of modeling requires that processes of photosynthesis (carbon dioxide capture and fixation to form organic carbon, releasing molecular oxygen in the process) and transpiration (evaporation of water from leaf tissue) are well-characterized from as much fossil morphological, geochemical, and molecular phytochemical evidence as possible. This paper examines the ecophysiological, paleobotanical, and paleoenvironmental consequences of refining our understanding of a key fossil plant group, the pteridosperm order Medullosales (medullosan seed ferns). It will further consider the importance of this refined understanding for reconstructing the influence of Pennsylvanian vegetation on global climate through the hydrologic cycle.

Plants and water

At local and regional scales, plants exert important effects on the environment through the absorption and fixation of carbon dioxide into organic carbon in exchange for water evaporated from leaves. During transpiration, a tension is generated within leaves that draws water up from the soil, into roots, through a network of dead, lignified, hollow cells (xylem), to the site of evaporation, allowing the plant to continue exposing its hydrated interior to the drying power of the atmosphere. Some of this water is oxidized as an electron donor for photosynthesis, releasing molecular oxygen in the process. However, more than 95% of the water that passes through a plant during its lifetime is lost through stomata, thus permitting the absorption of carbon dioxide. The processes of transpiration, assimilation, and the activity of photosystem II producing atmospheric oxygen, therefore play key roles in the local, regional, and global hydrologic, carbon, and

oxygen cycles, over short and long timescales.

The supply of water exchanged via evaporation from within leaves is determined by a number of factors, including local water availability (soil water potential), the rate of water transport through the plant to the leaves, the individual hydraulic capacity of the stems and leaves (how much water they can hold), and the evaporative demand placed on leaves by atmospheric conditions. Plants behave in a manner similar to a capacitor, where storage of water in the living tissue slows conductance in the soil-plant-atmosphere continuum (SPAC; Gleason et al., 2014). The evolution of cells and tissues specialized for the maintenance of homeohydry (i.e., the capacity of plants to regulate homeostasis of cell and water content) was essential to the success of early land plants, allowing them to photosynthesize and moderate water loss in the relatively dry atmosphere.

Within the SPAC, the characteristics of the plant-canopy boundary layer and the soil water potential are extremely important for determining a plant's water use under a given climate. In the soil, water availability is governed by soil depth, texture, and structure, which determine soil porosity and permeability, and by the depth of wetting of that soil. Because most roots of modern plants are concentrated in the upper 50 cm of the soil (Canadell et al., 1996), infiltration and percolation of water through the soil affect the degree to which roots intercept that moisture and are exposed to saturated conditions. Evidence from Middle Devonian (Givetian) *Eospermatopteris* forests showing rooting depths of >1m indicate that early in their evolution, land plants were well adapted to exploiting soil resources (Mintz, et al., 2010). Soil texture and structure affect plant water availability due to electrochemical binding of water molecules to soil particles and by creating pore spaces. This binding negates some of these hydrostatic forces of pore water and gravity, and gives rise to a pressure force (matric potential) that plants must overcome to move the water from soil across the root cell membrane. Plants accomplish this by lowering the osmotic potential through production of polar, non-metabolic solutes within the root cells. Generally, this potential ranges between -0.4 to -2.5 MPa (megapascals; 1 MPa = ~10 atm), with the lower value a critical threshold for damaging the cell. Different-sized particles and electrochemical properties of some soil minerals affect this process. Generally, larger-sized

particles, such as sand, increase pore size and have limited interaction with the bipolar water molecule, making water more available per unit volume in sandy soils as compared to soils enriched in smaller particles and with poor soil structure. Clay particles have small pore sizes that increase binding of water from capillary forces, and have charged surfaces that also retain water. The degree of wetting and drying of soils from precipitation and drought also are affected by these soil properties, leading to long-term effects on water availability and, thus, plant water use and productivity. The topographic position of a plant within a landscape is another significant influence on water availability: plants may receive surplus water via downhill and lateral transmission through soils.

Air boundary layers may have effects on water transport at several different spatial and temporal scales. The boundary layer is a zone of laminar flow that forms between any solid surface and the turbulent air flow that surrounds it; in the case of a leaf, the thickness of this layer, which is a function of both leaf size and the intensity of surrounding turbulent flow, reduces water flux from the leaf by slowing evaporation and movement of transpired gases away from the leaf surface. At fine scales, a leaf may have a boundary layer of still air very near the surface of the leaf. The thickness of this air layer affects the rate at which gas and energy exchange to and from the leaf occurs. Large leaves have larger boundary layers because the higher surface area increases the amount of non-turbulent wind flow over the leaf. Leaves with rippled surfaces or epidermal projections (e.g., trichomes) increase the amount of turbulent flow and reduce the boundary layer, and sunken stomata or stomata with papillae can increase the boundary layer near the stomata. Even under fairly moist conditions, the water potential of the air within the leaf boundary layer may be -100 MPa. Similarly, at the canopy scale, a monoculture, even-aged stand of trees may be aerodynamically smooth with a deeper boundary layer than a stand of mixed species or of different heights. Stands with gaps and trees with variable height increase turbulent airflow over the canopy, increase air mixing, and increase overall conductance.

At a planetary scale, the atmospheric boundary layer defines the lowest portion of the atmosphere that is in direct communication via gas, energy, and momentum exchange with the surface, and separates the surface from the free

atmosphere. Mixing within the atmospheric boundary layer occurs through turbulence, which is predominantly influenced by wind shear and convective instability. By enhancing evapotranspiration and moistening of low-level air, plants provide latent heat to the atmosphere that fuels deep convection and enhances surface-to-atmospheric mixing. Where evapotranspiration is limited, sensible heat may build at the surface with limited vertical mixing, leading to a larger, warm, dry boundary layer.

Plant organs and plant physics

The same basic physical and biochemical processes operate in all embryophytic plants to maintain adequate tissue water, assimilate carbon dioxide, and biosynthesize structural carbohydrates. All plants employ the same or similar biochemical substrates; they respond to the same environmental physics using the same physiological processes; and face the same tradeoffs (e.g., the water-transport morphologies that maximize flow volume also minimize safety; Tyree and Zimmermann, 2002). However, a distinction must be drawn between the maximum theoretical function of a plant and its actual operational performance. Examining individual organs or cells within a plant can help determine the former, but only by integrating the whole plant as a functioning organism can the latter be determined. For simplicity, plant organs are treated in order from best to least studied (from the perspective of the fossil record): stems, leaves, and roots.

Stems

Vascular plants are divided into two discrete categories based on the types of tracheary elements that form the water-conducting part of the stem xylem. The first group are plants with vascular systems formed of tracheids (lycophytes, ferns, gymnosperms, and the “vessel-less angiosperms”), which are narrow, tapered cells with only pit connections between cells. The second group contains those plants with vessels formed from vessel elements (primarily among angiosperms), which are generally larger in diameter than tracheids and, in addition to pits, have perforated end walls that lack a primary wall, allowing minimally restricted water flow between cells lined end-to-end vertically. For most plants, the largest volumes of water flow through xylem that develops later in ontogeny, either metaxylem or secondary xylem. Metaxylem

is a primary tissue derived from the apical meristem, matures later in development. Secondary xylem derives from the vascular cambium. There are a wide variety of stem xylem topologies, including novel combinations in hydraulics and biomechanics that are known only from extinct plants (Rowe et al., 1993; Rowe and Speck, 1998, 2004, 2005; Masselter et al., 2007).

Plant water transport is limited by the entry of air into the water transport system, a process called cavitation, and the subsequent expansion of those air bubbles to block individual xylem conduits, called embolism. When embolized conduits interrupt the pipeline of water to the leaves, stomata will close, photosynthesis will stop, and the leaves will eventually die (Taiz and Zeiger, 2002). Individual plants frequently experience embolism events, and resistance to cavitation can be an important component of individual plant, intraspecific, and interspecific competition (Hacke et al., 2000; Tyree and Zimmermann, 2002). Embolism is important on the ecological scale because it controls plant presence/absence, and can be used to set environmental limits on individual plant ecotypes (e.g., Pockman and Sperry, 1997, 2000).

Above-ground plant stems are vulnerable to cavitation via the entry of air through cortical tissues and into the transpiration stream (“air-seeding”) through pit membranes in tracheary elements, which can be weakened by a variety of factors, including cavitation fatigue, bacterial and fungal attack, age-related degradation, and more (Tyree and Sperry, 1989). The precise relationship between xylem anatomical features and cavitation resistance is a result of a number of complex factors, including biomechanics and whole-plant xylem architecture, but pit-membrane structure appears to be a major, if not the central, anatomical feature that determines cavitation resistance (Hacke et al., 2000, 2007; Sperry, 2003; Wheeler et al., 2005; Choat et al., 2006; Pittermann et al., 2006, 2010, 2011; Sperry et al., 2006, 2007; Choat and Pittermann, 2009; Christman et al., 2009; Brodersen et al., 2014). Embolism vulnerability appears to be most closely related to two factors: the leakiness of pit membranes with respect to air (pit membranes with larger pores permit air bubbles to pass through more easily), and the frequency of pits on a tracheary element (more pits on a tracheary element increases the probability of rare, very leaky pits). However, it should be noted that the process of air-seeding and subsequent cavitation

is the result of a complex series of chemical, mechanical, and anatomical interactions in the xylem, much of which is actively under investigation (Rockwell et al., 2014). Where pit membranes can be imaged and measured from living plants or the fossil record, a variation of the capillarity equation can be used to estimate the pressure at which an air bubble could pass through the pit membrane (e.g., Choat et al., 2003, Rockwell et al., 2014), which is one way to estimate the cavitation resistance of an individual tracheary element.

Mathematically, long-distance water transport through stem xylem is, essentially, pressure-driven flow through a plumbing network with individual pipes that each confer some hydraulic resistance to flow. Since the late 1940s, standard methods to quantify hydraulic resistance have analogized flow through xylem to Ohm’s Law, which equates the flow of current across a circuit to the quotient of the voltage drop divided by the electrical resistance of the circuit (van den Honert, 1948). According to this analogy, the flux of water through a plant is a function of the pressure drop across the plant (air-to-soil water potential gradient) divided by the hydraulic resistance to flow through tracheary elements. Because the water potential gradient will vary in accordance with environmental conditions (air temperature, relative humidity, soil water potential), it is often convenient to compare the hydraulic resistance of different plant species (Sperry, 1986, 2000, 2003; Tyree and Sperry, 1989; Comstock and Sperry, 2000; Hacke and Sperry, 2001; Pittermann et al., 2005; Sperry et al., 2005, 2007; Hacke et al., 2006). Individual species’ hydraulic resistances are a function of xylem anatomy and can be derived from tracheary element morphologies preserved in the fossil record. A number of extremely useful texts have been produced that discuss, in detail, aspects of the hydraulic resistance of individual plants, including papers with emphasis on key parameters involved and nomenclature (Zimmermann, 1983; Sperry, 1986, 2003; Sperry and Tyree, 1988; Tyree and Sperry, 1989; Tyree and Ewers, 1991; Comstock and Sperry, 2000; Hacke and Sperry, 2001; Sperry et al., 2002, 2005, 2006, 2007, 2008; Tyree and Zimmermann, 2002; McCulloh and Sperry, 2005; Hacke et al., 2006; Choat et al., 2008; Jansen et al., 2009; Melcher et al., 2012).

One way of standardizing measurement of hydraulic resistance and inverting to quantify

hydraulic conductance is through single-conduit analysis. In these analyses, anatomical properties of individual cells are modeled, followed by normalization to cell dimensions (e.g., cross-sectional area), thus permitting different plant taxa to be compared: living vs. extinct, tropical vs. temperate, etc. Key papers have laid out the justification and background for this type of analysis (Lancashire and Ennos, 2002; Hacke et al., 2004; Sperry and Hacke, 2004) and were further developed for use on plant fossils (Wilson et al., 2008; Wilson and Knoll, 2010; Wilson and Fischer, 2011; Wilson, 2013).

Single-conduit analyses decompose the hydraulic resistance of a cell into two components: the hydraulic resistance from the lumen, and resistance from the walls. Within the tracheary element wall, the major components are the pit membrane, and the aperture. Pit membranes and apertures can be parameterized in different ways (Lancashire and Ennos, 2002; Hacke et al., 2004; Sperry and Hacke, 2004; Wilson et al., 2008; Wilson and Fischer, 2011) depending on the morphology of the pit found in the conduit.

Analysis of the hydraulic resistance of living-plant conduits, in tandem with detailed anatomical investigation, has established some useful guidelines for how hydraulic resistance is partitioned between the lumen and the pits. Most measurements, regardless of taxon or method involved, suggest that the resistance is 60%–40% or 40%–60% wall/lumen resistance, depending on the size of the conduits involved (Wheeler et al., 2005; Choat et al., 2006, 2008; Sperry et al., 2006; Pittermann et al., 2010, 2011; Brodersen et al., 2014). SEM analysis of pit membranes and experiments have suggested that for the homogeneous pit membranes of angiosperms, the pores are on the order of 30 nm in diameter, but possibly wider if the overall resistance partitioning relationships have to be satisfied.

In fossil plants, stem hydraulic-conductivity values can be calculated using models seeded by conduit dimensions observed through transverse, tangential, and radial sections, which provide diameter and length values, and radial, tangential, and SEM views of pit dimensions and frequency from individual cells (Wilson et al., 2008; Wilson and Knoll, 2010; Wilson, 2013). The most challenging parameter to obtain from fossil material is conduit length because both ends of a single tracheary element are rarely observed in thin-section views of fossil plants, given the

three-dimensional nature of xylem and the two-dimensional view provided by a thin section. If the plant is preserved in carbonaceous material, gentle maceration of stem xylem with weak acids (e.g., 1N HCl) is often sufficient to expose individual cells, which can then be measured using light microscopy. Statistical methods can also be used to estimate tracheid length given a distribution of tracheid sizes within a fossil (Cichan and Taylor, 1985; Baas et al., 1986; Wilson and Fischer, 2011a). However, the diameter and pit attributes (number, morphology, membrane porosity) of a tracheary or vessel element play a greater role in determining the overall hydraulic resistance of a single cell.

Scaling up from cells to tissues to trees remains a challenge (Sperry et al., 2008) but many general observations can be made. First, wider and more pitted cells have a significantly lower hydraulic resistance and can permit the passage of more water for a given water-potential gradient. Second, longer cells also have a lower hydraulic resistance compared with cells of equivalent diameter and pit frequency; additionally, they confer lower hydraulic resistance on the whole plant because water will cross fewer end walls and pit membranes. Finally, pit distribution and connectivity can spread embolism throughout the plant; therefore tracheary elements or vessels that are more pitted and have more overlap can spread embolisms more easily (Loepfe et al., 2007).

Leaves

Leaves are the plant organs that serve as the most dynamic interface between the plant and the atmosphere. On most plants, leaves are the sole sites of stomata, which are discussed in detail below. From the perspective of water and plants, leaves are important because they are the terminal location in the pathway of water from the soil to the atmosphere. The supply of water to leaves is of critical importance for plant growth: in most temperate angiosperm plants, more than 300 molecules of water are evaporated from the leaf for every molecule of carbon dioxide fixed through photosynthesis (Taiz and Zeiger, 2002). Xylem enters the base of a leaf as part of a vascular bundle and forms a pathway through the petiole to the leaf surface, whereupon the xylem is dissected into smaller and smaller networks of xylem cells, the veins. When stomata are open, water is drawn from the veins and toward the substomatal chamber via the apoplastic pathway:

through the cell walls of photosynthetic cells.

Increasing evidence has pointed to the distribution of leaf xylem (in the form of veins) as placing fundamental constraints on gas exchange and plant growth. Both experimental analysis of a diverse range of land plants (Brodribb et al., 2007) and synthetic models of leaves (Noblin et al., 2008) have indicated that the maximum photosynthetic rate in plants is set by the spacing of leaf veins. Related work has demonstrated the importance of the hydraulic pathway in leaves, which can contain high hydraulic resistances; the final portion of the pathway, between leaf veins and the substomatal chamber, may account for 90% of the hydraulic resistance in certain leaves (Sack and Holbrook, 2006).

Many recent studies have supported ecophysiological principles based upon the physical architecture of veins within leaves; plants with veins that are closer to one another and are short distances from substomatal chambers can supply a higher flux of water for evaporation and can do it more quickly than plants with few veins, widely separated veins, or large veins within massive leaves (Brodribb et al., 2007; Boyce et al., 2009, 2010; Feild et al., 2011). This capacity to support high water loss—leaf hydraulic capacity, or K_{leaf} [$\text{mmol H}_2\text{O} / (\text{m}^2 \cdot \text{s} \cdot \text{MPa})$ —is inversely related to the maximum distance that water travels from veins to stomata through the mesophyll, or D_m [μm] (Brodribb et al., 2007); leaves with veins close to stomata can supply more water for evaporation, whereas leaves with veins far from stomata cannot support a high demand and therefore have a lower K_{leaf} . Leaf hydraulic capacity (K_{leaf}) is related, in turn, to the maximal photosynthetic rate of the plant; higher K_{leaf} values facilitate more photosynthesis, whereas lower K_{leaf} values rule out high photosynthetic rates. One major result from this work is that every group of land plants with stomata, from bryophytes to angiosperms, appears to obey the physical relationship between leaf architecture, hydraulic capacity, and photosynthetic rate, simply because of the physics of plant water transport (Brodribb et al., 2007; Feild et al., 2011).

Studies of extant plants suggest the possibility of reconstructing leaf hydraulic capacity directly from fossil material if the three-dimensional structure of the leaf is known. If the fossil material is well preserved, serial transverse sections through leaves will allow the distance between the abaxial edge of the leaf vein and the

substomatal chamber to be measured (Fig. 1 C, D). With multiple leaves and multiple measurements, a range of D_m values can be produced. In many lycophytes and ferns, D_m values $>500 \mu\text{m}$ have been measured; for some angiosperms, distances as short as $100 \mu\text{m}$ have been documented (Brodribb et al., 2007). Among extinct lineages, D_m values resemble those found among living relatives, with the exception of the pteridosperms (see below).

A closely related, but not identical, parameter that has been employed to study the physiology of living and extinct plants is vein density (Boyce et al., 2009, 2010; Feild et al., 2011). Vein density, or vein length per area, is the amount of leaf vein that can be measured within a given area of leaf tissue, typically expressed in units of [mm^{-1} or mm mm^{-2}] but alternatively, and perhaps more clearly, as [$\text{mm vein per mm}^2 \text{ leaf}$]. Measuring vein density in fossil and living plant material is straightforward: top-down views of leaves are generated, and overlain with a square grid (for example, $3\text{mm} \times 3\text{mm}$). Within this grid, all visible veins are traced and their length is totaled, expressed as a function of the grid area (9mm^2 , in this example). One advantage to investigating venation architecture broadly, and vein density in particular, is that vein density is easy to measure in fossil material, does not require anatomical preservation to be measured, and values can be derived from compression fossils (e.g., Boyce and Knoll, 2002; Fig. 1 A, B).

Although vein density and vein-to-stomata distance are closely related proxies of leaf potential to release water vapor, the values are not identical: elevated leaf thickness, in particular, can result in high D_m values for high-vein-density taxa, and vice versa. For very thin leaves with a moderate vein density, which can be found within the pteridosperms, low D_m values, and consequently, high K_{leaf} values, can be measured.

Roots

Roots increase plant surface-area to soil-volume space, facilitating higher sustainable water and nutrient uptake in marginal habitats. The evolution of roots in land plants permitted enhanced water uptake and mineral absorption, and may have been critical to the evolution of the arborescent habit. Roots are considered to have emerged as a distinct organ type between 416 to 360 Ma, and almost certainly evolved independently in the lycophytes (and perhaps several times there) versus the rest of the vascular

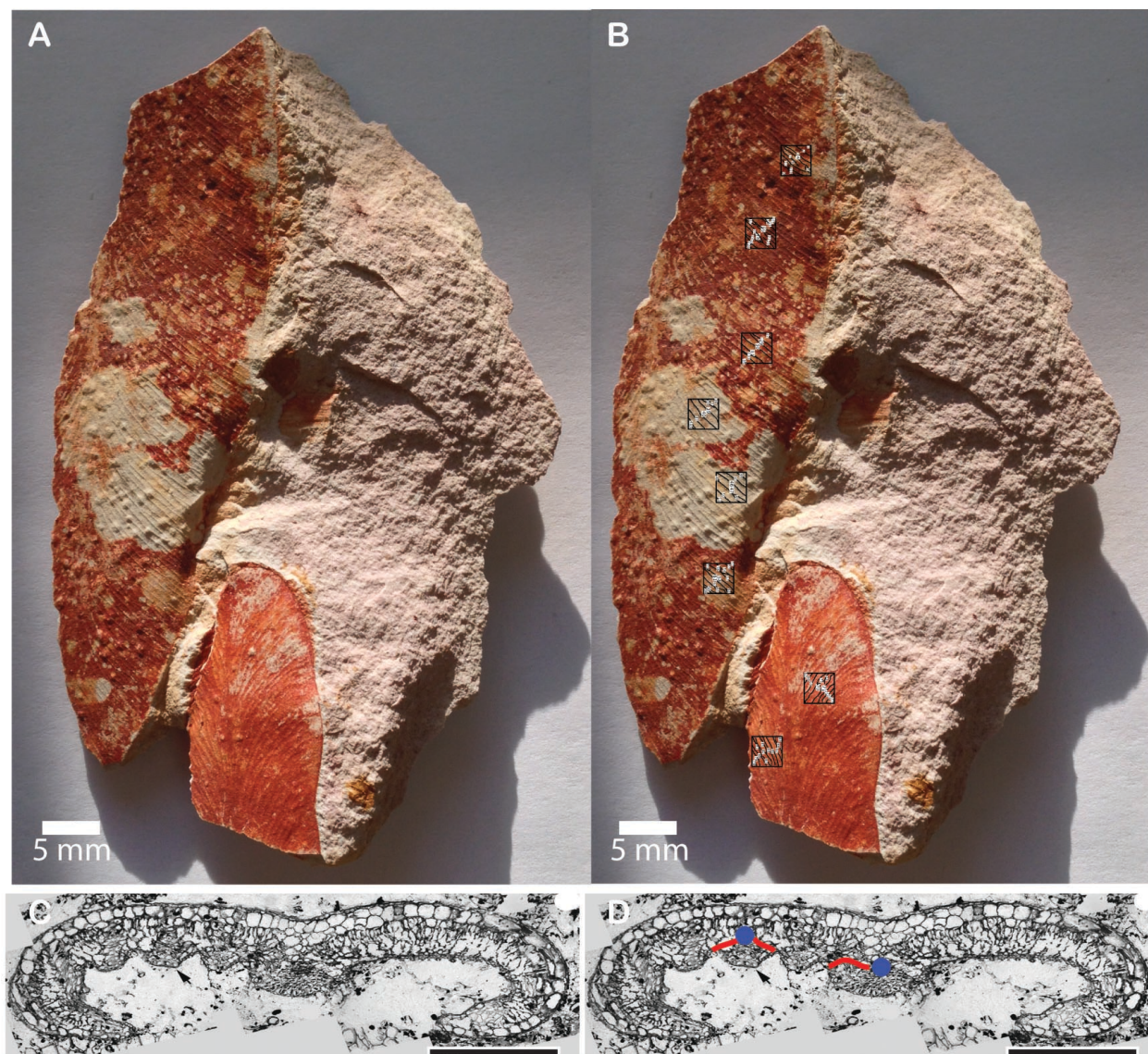


FIGURE 1.—(A, B) Measuring vein length per area (also described as vein density) in a leaf compression fossil of the late Paleozoic seed plant *Glossopteris* from the Sydney Basin, Australia (Haverford College Collection ID: AUS1). Scale bar = 5mm. A) Image of leaf fossil; note the dichotomizing veins. B) Image overlain with several 3mm x 3mm grids, veins traced and marked using the open-source program ImageJ. Several measurements should be made of each leaf in order to generate robust values, and, in the case of leaves with dichotomizing veins, measurements should be made distal to the midvein, if possible. (C, D) Cross-section image of a permineralized pinnule of *Alethopteris lesquereauxii*, described by Raymond et al. (2014). Reprinted from *Review of Palaeobotany and Palynology* v. 200, Raymond et al., “Permineralized *Alethopteris ambigua* (Lesquereux) White: A medullosan with relatively long-lived leaves, adapted for sunny habitats in mires and floodplains,” p. 82–96, © 2014 with permission of Elsevier. Scale bar = 1mm. C) Note thin size of the leaf; D) D_m distances illustrated in red.

plants (Raven and Edwards, 2001; Kenrick and Strullu-Derrien, 2014) In all plants except two groups of lycophytes, roots by definition include multicellularity, endogenous branching, evidence of root hairs, and presence of a root cap (Kenrick and Strullu-Derrien, 2014). In many, if not all, lineages of early land plants, mycorrhizal associations played a major role in facilitating

early acquisition of nutrients, and probably played a minor role in facilitating increased water uptake from soil environments (~4% increase from arbuscular mycorrhizal hyphae: Khalvati et al., 2005). Natural selection is presumed to have favored individuals with roots as competition for hydric environments intensified and increasing biodiversity and rates of productivity increased

intraspecific and interspecific competition. While embryonic development may have differed, both root forms facilitated higher levels of plant vascular “plumbing” throughout the soil, making more water available for the plant and allowing higher levels of water transpiration from the soil to the atmosphere (Algeo and Scheckler, 1998). A central stele, or bundle of vascular cells in the center of the root, is common to all seed plants of Pennsylvanian age.

From a quantitative perspective, root function operates under the same set of structure-function relationships as stems. Much like stem xylem cells, wide root xylem cells transport more water but provide less mechanical support, whereas smaller cells transport less water but enable mechanical stability and resistance to a variety of stresses. Therefore, the quantitative approaches taken to understand stem hydraulic function and evolution can, in theory, be applied to roots. However, roots are most often preserved in isolation from the above-ground plant body and can rarely be tied to specific plant morphologies, but exceptions are known (Rothwell and Whiteside, 1972), particularly for the stigmarian rooted lycopsids (e.g., Williamson, 1887). Future detailed study of Carboniferous rooting structures may help shed light on a number of environmental and biomechanical aspects of late Paleozoic plant biology, much like they have for key Devonian taxa, such as the progymnosperm *Archaeopteris* (Meyer-Berthaud et al., 2000).

Geochemical records of evapotranspiration

Carbon, oxygen, and hydrogen isotopes of leaf organic matter provide a geochemical record of specific leaf and environmental parameters at the time of molecular biosynthesis (Dawson et al., 2002). The carbon isotopic composition ($\delta^{13}\text{C}$) of leaves is determined by the carbon isotopic composition of the atmosphere and the ratio of the partial pressure of CO_2 at the site of carboxylation in the chloroplast and ambient air (c_i/c_a). The most commonly utilized model of carbon isotope discrimination during carbon fixation in C_3 plants describes the fractionation in plant material as:

$$\Delta = a(p_a - p_i)/p_a + b(p_i/p_a) = a + (b-a)(p_i/p_a) \quad \text{Eq. (1)}$$

where a is fractionation due to diffusion in air (4.4‰), b is the subsequent fractionation during carboxylation and isotopic discrimination by Rubisco, and p_i and p_a reflect the partial pressure of leaf internal and atmospheric carbon dioxide

(Farquhar, 1982; Farquhar et al., 1989a). In this parameterization, when stomatal conductance is small relative to CO_2 fixation capacity, p_i is small and Δ is reduced. When conductance is high, the internal pressure of CO_2 approaches p_a and Δ approaches the maximum isotopic discrimination controlled by Rubisco. Thus, the carbon isotopic composition of plant leaves reflects regulation of the stomata to balance carbon assimilation and net photosynthetic rate (A), and stomatal conductance (g_s) and water loss (Farquhar et al., 1989b; Dawson et al., 2002).

Because leaf stomatal conductance (g_s) and photosynthetic rate (A) both impact CO_2 partial pressure in the leaf, and thus p_i/p_a , carbon isotopic variations that are preserved in ancient leaves can reflect changes in either A or g_s (Keitel, 2007). Oxygen isotopes of leaf cellulose have been utilized to provide an additional tool for distinguishing between carbon isotope effects due to variations in A or g_s (e.g., Moreno-Gutierrez et al., 2012). This is because the oxygen isotopic composition of leaf water is believed to respond to changes in g_s in concert with carbon isotope changes, but is generally insensitive to changes in A (Scheidegger et al., 2000; Grams et al., 2007; Cernusak et al., 2008; Moreno-Gutierrez et al., 2011; Roden and Farquhar, 2012).

Variation in the oxygen and hydrogen isotopic composition of water in plants is controlled by the isotopic composition of water taken up by the plant, enrichment of leaf water during transpiration, mixing of enriched leaf water and unenriched source water, and isotopic exchange between biomolecules and water during biosynthesis (Barbour et al., 2004). The process of water uptake into the xylem produces minimal or no isotopic fractionation between ambient soil or groundwater and the plant (Barbour, 2007). However, photosynthetic carbon fixation requires the opening of stomata to allow CO_2 diffusion to carbon fixation sites, mediating water loss to the atmosphere. This process of water loss is accompanied by evaporative enrichment of residual leaf water O and H due to slower diffusion of the isotopically enriched water-vapor species (H_2^{18}O) relative to depleted water-vapor species (H_2^{16}O). The O and H isotopic composition of leaf water therefore reflects the degree to which leaf water is evaporated during the process of transpiration.

The H and O isotopic composition of leaf water present at the site of carbon fixation can be modeled using an approach that includes

equilibrium isotope effects related to the phase change from liquid to vapor during evaporation, and kinetic isotope effects that result from differences in the rate of diffusion of heavy and light isotopes of O and H as water vapor in air (Equation 2) (Craig and Gordon, 1965; Farquhar et al., 1989b; Flanagan et al., 1991; Flanagan and Ehleringer, 1991):

$$R_{wl} = a^*[a_k R_{wx}(e_i - e_s / e_i) + a_{kb} R_{wx}(e_s - e_a / e_i) + R_a(e_a / e_i)] \quad \text{Eq. (2)}$$

Subscript a = bulk air, k = kinetic fractionation factor, wl = leaf water, and wx = xylem water; e = vapor pressure of air (e_a), leaf surface (e_s), and intercellular air spaces (e_i); a^* is the temperature-dependent equilibrium fractionation for H and O between water vapor and liquid (Majoube, 1971), and a_{kb} is the kinetic fractionation associated with diffusion through the boundary layer. This kind of model generally oversimplifies processes in specific leaves because it assumes generally steady state. Furthermore, the model is less accurate when predicting bulk leaf water compared to water at the site of evaporation (Rodin and Ehleringer, 1999). However, this approach provides very good agreement between predictions of leaf water O and H isotopes at the site of evaporation, and provides an important tool for reconciling environmental parameters that impact leaf-water isotopic composition and, ultimately, the plant organic-matter composition.

In living plants, measures of the oxygen isotopic enrichment of cellulosic plant material relative to source water ($\Delta^{18}\text{O} = \delta^{18}\text{O}_{\text{plant}} - \delta^{18}\text{O}_{\text{source water}}$) are used to identify interspecific differences in stomatal conductance (g_s), due to the inverse relationship between $\Delta^{18}\text{O}$ and the ratio of atmospheric to intercellular leaf-water vapor pressure (Barbour, 2007; Farquhar et al., 2007; Moreno-Gutierrez et al., 2012). Increases in stomatal conductance should increase transpiration, which has the effect of producing increased evaporative enrichment of heavy oxygen and hydrogen isotopes in leaf water. Transpiration rates should increase when there is an increase in vapor pressure deficit (VPD) and/or stomatal conductance (g_s), because both factors affect leaf water volume, and therefore isotopic composition, in the same direction.

Studies of modern plants show a strong correlation between leaf intrinsic water-use efficiency (WUE_i), defined as (A/g_s), and $\Delta^{18}\text{O}$

(Gutierrez-Moreno et al., 2012) and cellulose $\delta^{13}\text{C}$ and WUE_i . The $\Delta^{18}\text{O}$ is observed to be strongly negatively correlated with stomatal conductance, while $\delta^{13}\text{C}$ is positively correlated with intrinsic water use efficiency (WUE_i). This relationship holds across a large number of phylogenetically distant plant-functional types providing a reliable indicator of g_s and WUE_i .

Over geologic timescales, plant organs can be fossilized with intact leaf architecture, structural molecules, and cuticular waxes. However, cellulosic material readily degrades over long timescales, limiting the ability to measure $\delta^{13}\text{C}_{\text{leaf}}$ and $\delta^{18}\text{O}_{\text{cellulose}}$ in tandem. Recalcitrant organic biomarkers form cuticular waxes that coat the surface of leaves, and are readily preserved with minimal or no isotopic exchange over geologic timescales and at temperatures of $<150^\circ\text{C}$ (Schimmelmann, 2006). The hydrogen isotopic composition of ancient cuticular waxes can provide much the same information of $\Delta^{18}\text{O}_{\text{cellulose}}$, although factors controlling the oxygen isotopic composition of organic matter are better constrained than those controlling hydrogen isotope compositions (Farquhar et al., 2007).

Normal alkanes are abundantly produced as epicuticular waxes on the leaf surface and aid in water repellency and protection from UV radiation or predation (Holloway, 1969; Barthlott and Neinhuis, 1997). Straight-chained n-alkanes and other compounds may be bound to clays in sediments, preserved as intact cuticle on fossil leaf materials in thermally immature sediments (as is the case with our sample sites), or occluded in secondary minerals. Whereas some complex biomarkers can be readily degraded, simple straight-chained n-alkanes can be preserved without isotopic exchange over geologic time (Schimmelmann et al., 1999; 2006; Hren et al., 2010) and provide an ideal target for constraining paired compound-specific carbon and hydrogen isotope compositions that record environmental parameters at the time of biosynthesis. If paired with other proxies for ground or stem water, these should, in theory, provide a record of WUE_i and g_s , similar to modern $\delta^{13}\text{C}$ and $\Delta^{18}\text{O}$.

Stomata and the environment

There is a rich literature on stomatal modeling, but most analyses and models that involve fossil plant stomata emphasize the interaction between the morphology and density of stomata on a leaf's surface with relation to environmental conditions such as irradiance (Lake et al., 2001), water

availability (Edwards et al., 1998), and atmospheric and carbon dioxide (Woodward, 1987; Malone et al., 1993; Woodward and Kelly, 1995; McElwain and Chaloner, 1995; Wagner et al., 1996; Royer et al., 2001; Kurschner et al., 2008; Konrad et al., 2008; Barclay et al., 2010; Haworth et al., 2013; Dow et al., 2014; Franks et al., 2014). Over evolutionary timescales, the evolution of particular stomatal characteristics have tended to be linked with increasing internal leaf exposure to CO₂, while less emphasis has been placed on the role of stomatal characteristics' effects on water retention and driving long-distance water transport throughout the entire plant (Raven, 2001). Fewer studies have considered how stomatal density and size can influence water loss from leaves (Steinhorsdottir et al., 2012), yet this is an important consideration because transpiration can account for ~60% on average of the total evapotranspiration budget and returns ~39 ±10% of incident precipitation back to the atmosphere (Schlesinger and Jesechko, 2014). When reconstructing whole fossil plant paleophysiology, it is important to integrate data from stomata on leaves with that of root, stem, and leaf xylem conductivities.

With respect to water, stomatal dimensions determine the maximum stomatal conductance rates. The morphologic characters of guard cells affect both maximum opening size of the stoma (a_{\max} ; m²) and the depth of the stomatal pore (l ; m). Density, or frequency, of guard cells (D ; m⁻²) can be controlled by genes expressed during water loss due to transpiration and increased production of drought-specific hormones (Casson and Hetherington, 2010; Kuromori et al., 2014). Pairs of guard cells ultimately give rise to stoma in which the maximum conductance of water vapor ($g_{w\max}$; m s⁻¹) may be estimated by:

$$g_{w\max} = [(d/v) * D * a_{\max}] / [l + (\pi/2) * \sqrt{(a_{\max}/\pi)}] \quad \text{Eq. (3)}$$

Where d_w is the diffusivity of water vapor in air (0.000249 m² s⁻¹ at 25°C) and v is the molar volume of air (0.0224 m³ mol⁻¹ at 25°C). This generalized equation can be modified to account for different shapes of the stomatal pore, which are likely to be important as a phylogenetic constraint (Hetherington and Woodward, 2003). For example, a_{\max} is maximum stomatal pore area (m²) calculated as an ellipse using stomatal pore length (length in m) as the long axis and 1/2 as the short axis (if following a gymnosperm stomatal

pore geometry; Franks and Farquhar, 2007) or as a circle with a radius equal to 1/2 (if following an angiosperm stomatal pore geometry; Franks and Farquhar, 2007). The stomatal pore depth, l (in m), is considered to be equivalent to the width of an inflated, fully turgid guard cell (Franks and Beerling, 2009).

Once a satisfactory maximum conductance value is derived from characteristics drawn from literature or fossil values, operational conductance must be considered. Various methods exist to estimate the actual conductance of a plant; however, most of the models used to estimate actual conductance consider a scalar reduction of $g_{w\max}$ utilizing estimate of soil water, temperature, and precipitation limits, or assume a coupled photosynthetic-transpiration relationship in which the conductance is ultimately limited by the carboxylation rate of photosynthesis and by the need to maintain internal levels of CO₂ (Damour et al., 2010). Because limited information is available from paleoproxies on either climatic constraints of conductance or in-vivo rates of photosynthesis of extinct plants, $g_{w\max}$ is often used as a starting point for estimating maximum water use by plants and a proxy for potential of plants to release water through the SPAC based on morphology.

Stomatal density (SD) has been widely used as a proxy to reconstruct paleo-CO₂ concentration because modern experimental and recent historical studies demonstrate a strong inverse relationship between SD and CO₂ concentration (Woodward, 1987, 1993; Beerling and Chaloner, 1993; Beerling et al., 1993, 1998; McElwain and Chaloner, 1995, 1996; Kurschner et al., 1996). CO₂ sensors, CO₂ sensitive genes, and signaling pathways all play a role in the spacing of neighboring stomata, and therefore SD, and have been identified in the model plant *Arabidopsis* (Pillitteri and Dong, 2013). These observations suggest that there is a genetic basis underpinning how plants control the number of stomata that develop on the leaf surface in response to atmospheric CO₂ concentration, which ultimately controls how plants optimize carbon use against water loss. The inverse relationship between SD and CO₂ is not universal (Haworth et al., 2013), however, because some species show no stomatal developmental response to CO₂, whereas others show a positive relationship between SD and CO₂, contradicting the predictions of optimization theory. The most likely explanation for the diversity of SD responses to CO₂ among species

is that there is a tradeoff in the method by which plants can control CO₂ uptake and water loss (Haworth et al., 2013): some species control stomatal conductance rates (g_s) via modifications to stomatal size and/or density (e.g., the fern *Osmunda regalis* and the gymnosperm *Ginkgo biloba*), whereas others show little morphological plasticity in SD and stomatal pore size (e.g., the cycad genus *Lepidozamia*) and instead control g_s via physiological control of guard cell turgor pressure, which alters the dimensions of the stomatal pore. Despite differences in morphological and/or physiological mechanisms by which species control gas exchange, the maximum theoretical rates of water loss (g_{wmax}) for all species, extant and extinct, can be calculated according to the diffusion equation (Equation 3) (Parlange and Waggoner, 1970; Franks and Beerling, 2009). Maximum theoretical stomatal conductance to CO₂ uptake can, therefore, also be calculated by scaling g_{cmax} to g_{wmax} . Previous work (Farquhar and Sharkey, 1982) suggests that $g_{cmax} = (g_{wmax} / 1.6)$. Therefore, according to the theoretical relationships laid out by Eq. 3, high stomatal densities, large stomatal pore sizes, shallow pore depths or some combination of these attributes measured from fossil leaves will indicate that a fossil taxon has a high potential for water loss from its leaves.

Prevailing environmental conditions at any given time during the lifetime of the leaf will determine what proportion of the theoretical maximum conductance will be achieved. Drought, for example, will induce stomatal closure, whereas optimum field conditions for photosynthesis in relation to water, light, and nutrients will encourage stomatal opening. Recent studies seeking to assess the proportion of actual stomatal conductance (termed g_{op}) to g_{wmax} indicate that, on average, species tend to use 20% to 30% of g_{smax} in optimum field conditions irrespective of the phylogenetic group investigated (Dow et al., 2013; Franks et al., 2014; McElwain et al., 2015). These results are encouraging because they open up the opportunity to infer the rate of operational stomatal conductance to water in fossil plants from measurements of stomatal density, pore size and guard cell widths using $g_{op} = g_{wmax} * 0.2 \pm 0.1$. This will allow extinct taxa such as the medullosans to be placed in the same ecophysiological context of extant plants through their stomatal morphology, and will permit

assessment of their role in forcing the hydrological cycle through both maximum and operational stomatal conductance values.

Outstanding questions and other issues of plant physics

It is worth noting that there are some outstanding questions regarding the morphology of extinct plants and other issues of plant physics that deserve further attention. There are a number of plants, including many angiosperms (e.g., grapevine, *Vitis*) and some conifers (e.g., Douglas fir, *Pseudotsuga*) (Brodersen and McElrone, 2013), that are able to overcome environmental limits (e.g., water availability) by refilling embolized xylem conduits (Sperry et al., 1994; Salleo et al., 1996; McCully, 1999; Tyree et al., 1999; Hacke et al., 2001; Clearwater and Clark, 2003; Hacke and Sperry, 2003; Sperry, 2003; Stiller et al., 2005; Scheenen et al., 2007; Zwieniecki and Holbrook, 2009; Brodersen et al., 2010; Secchi and Zwieniecki, 2011). Plants that are capable of refilling embolized xylem conduits may have more plastic environmental tolerances than a simple anatomical analysis would suggest. Unfortunately for paleontologists, it appears that refilling capability leaves no unambiguous anatomical or geochemical marker that can be read directly from fossil plant anatomy, except for the observation that living cells within xylem, specifically ray cell parenchyma, appear to play a major role in some plants that are capable of refilling. However, wide rays are also characteristic of a number of plants with a lianoid habit, some of which have the ability to refill embolized vessels (e.g., grapevine, *Vitis*), which can confound a refilling interpretation based on the presence of wide rays alone. Therefore, plants with secondary xylem containing abundant rays may have had the ability to refill embolized xylem tracheary cells; and it is worth noting that this anatomical configuration is found in some Paleozoic woody plants, including the medullosans. Without an unambiguous refilling indicator, however, testing these hypotheses remains challenging.

Finally, the disarticulation of plant organs from a whole plant during life, and almost always upon death, will always be a challenge for reconstructing the total functional path-length of water in extinct plants. Precisely how many leaves were functional at a given time, or how much root surface area was supporting an individual plant, may remain unknown for a great

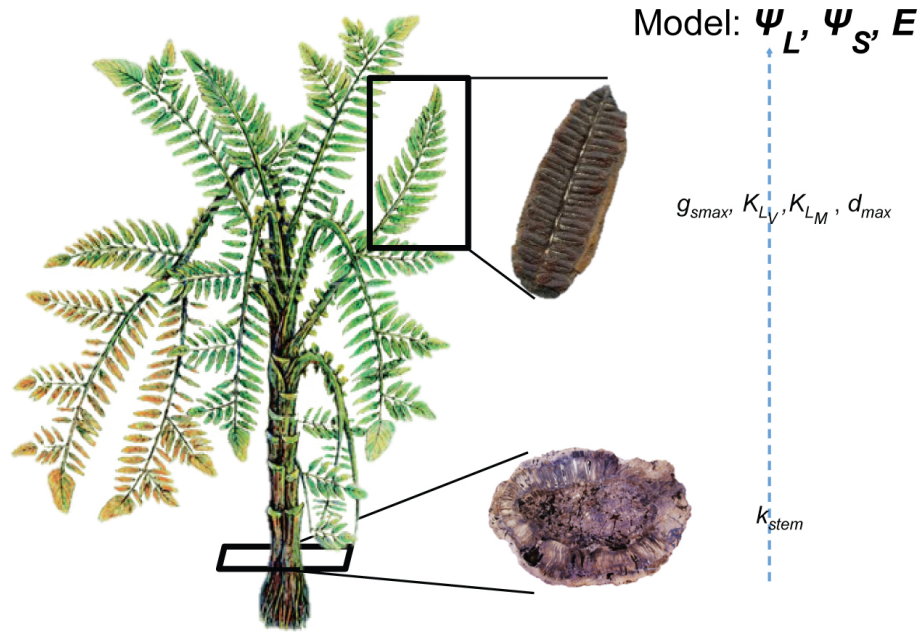


FIGURE 2.—Whole-plant reconstruction of a medullosan along with key parameters for quantifying its physiology, including maximum stomatal conductance to water (g_{wmax}), stem hydraulic conductance (k_{stem}), and evapotranspiration (E). See text for details.

number of extinct plant lineages. However, exceptional preservation of fossils, in particular those permineralized early in their burial, such as Carboniferous coal balls, has greatly facilitated the understanding of the morphology and ecology of several Paleozoic Era plant lineages, including the one investigated here: the medullosan pteridosperms, or seed ferns. Combining analysis of stem hydraulic conductivity (k_{stem}) with leaf physiological traits (g_{smax} , vein conductivity [K_{Lv}], mesophyll conductivity [K_{Lm}], and D_v) can lead to whole-plant parameters that are key to ecosystem modeling (Fig. 2).

CASE STUDY: THE MEDULLOSAN “SEED FERNS”

Fossil record of medullosans

Among late Paleozoic seed plants, a frequently occurring, yet physiologically puzzling, lineage is the medullosan pteridosperms, or medullosan seed ferns, so named because they, along with a number of extinct stem-group seed plants all placed in Division Pteridospermophyta, possessed fern-like fronds with large seeds attached (Scott, 1899, 1914; Galtier, 1988). Detailed analysis of medullosan reproductive structures, particularly the integuments of the ovules, has suggested to some authors an affinity with the cycads (Stewart and Delevoryas, 1956; Dennis and Eggert, 1978;

Eggert and Rothwell, 1979; Mapes, 1979; Stidd, 1981; Crane, 1985; Pryor, 1990; Drinnan and Crane, 1994; Nishida, 1994; Serbet et al., 2006); however, current analyses of the phylogenetic relationships among living seed plants, when combined with fossils, implies a topology that places medullosans as sister group to all living gymnosperms (Doyle, 2006; Hilton and Bateman, 2006; Fig. 3). The analysis presented here is agnostic on the precise placement of the medullosans within seed-plant phylogeny.

Medullosan anatomy and morphology is unusual, and has been noted as unusual since the early 19th century (Brongniart, 1828). The photosynthetic structures of medullosans were many-times-pinnate fronds (Fig. 2) that varied in length from approximately a meter (Laveine and Behlis, 2007) to over 5 meters (Laveine, 1987); large in length relative to the small stem area, in particular (see below). There were a large number of species and genera with a variety of morphological variations on this basic architecture (Wagner, 1968; Cleal and Zoderow, 1989; Cleal et al., 1990; Laveine and Dufour, 2012). Key genera for medullosan leaves include *Neuropteris*, *Alethopteris*, *Macroneuropteris*, *Neurodopteris*, and *Laveineopteris*, but others have been described (Taylor et al., 2009). Two key leaf genera can be distinguished easily. *Alethopteris* has relatively robust construction

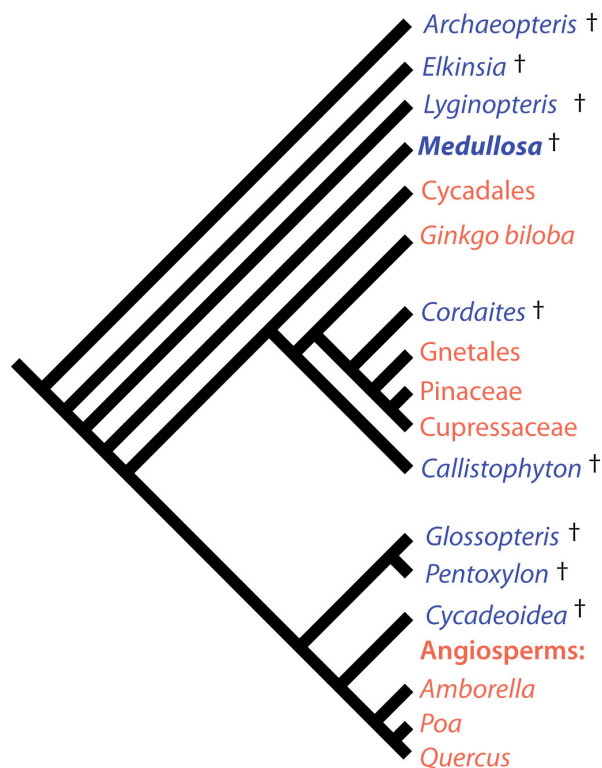


FIGURE 3.—A phylogenetic tree of extant and extinct seed plants, with the medullosans highlighted. Extinct plants are indicated with crosses. Topology of the tree is based on Doyle (2006). Note the phylogenetic distance between *Medullosa* and some of its closer physiological analogues, including the monocots, here represented by the genus *Poa*.

(Figs. 4A, 5C) and fronds can be quite large (Laveine 1987), leading to the conclusion that the plants, and their individual leaves, were relatively long-lived, with some species dwelling mainly in swamp habitats (Raymond et al., 2014). *Neuropteris* (and its closely related form genus, *Marconeuropteris*), had relatively thin and cheaply constructed laminate portions of their foliage (Fig. 4), perhaps indicating a short leaf lifespan, and fronds could vary greatly in size (Fig. 5A). Neuropterids are associated with a wide variety of environments, including stream margins, swamps, and overbank environments, leading to the interpretation that some species were fast-growing (Pfefferkorn et al., 1984; Wnuk and Pfefferkorn, 1984). Most medullosan leaves had open dichotomous venation, with a few notable forms characterized by reticulate veins. Typical medullosans also had large stomata, trichomes, or other specialized defense mechanisms (Fig. 5F), and many bore specialized structures that facilitated an obligate or facultative

climbing habit (Krings et al., 2003).

Medullosan stem anatomy is singular because its secondary development yields a series of discrete vascular segments within a single stem (Fig. 4C), giving the appearance of a plant that evolved through fusion of independent axial structures, which was an early hypothesis for its development (Delevoryas, 1955). This peculiar development of vascular tissue has been extensively investigated and remains a synapomorphy for the medullosan clade (Scott, 1899; Steidtmann, 1937; Andrews and Kernen, 1946; Stewart, 1950; Stewart and Delevoryas, 1952, 1956; Andrews and Mamay, 1953; Basinger et al., 1974; Mapes and Rothwell, 1980; Stidd, 1981; Pfefferkorn et al., 1984; Hamer and Rothwell, 1988; Pryor, 1990; Cleal and Shute, 2003; Dunn, 2006; Krings and Kerp, 2006; Krings et al., 2006; Wilson et al., 2008; Stull et al., 2012). These vascular segments anastomose throughout medullosan stems, providing complex and redundant (in the physical sense) pathways for water to the sites of evaporation in the leaves (Fig. 5E). Surrounding the eustele and the attendant cylinders of secondary xylem surrounding the eustelar bundles, located in the central region of a medullosan stem, is a variably thick band of cortical tissue (Fig. 5D,E) with a characteristic “spotted” texture. The cortex and bases of the large medullosan fronds can account for more than two-thirds of the cross-sectional area of a medullosan plant (Stewart and Delevoryas, 1952), and there is some geochemical evidence that suggests that the cortical tissues may have been softer and formed from cells without extensive lignification of their cell walls (Wilson and Fischer, 2011). Finally, the complex stem organization of medullosans reaches its apex in the larger, later medullosans: *Colpoxylon* (Fig. 4F) and *Medullosa stellata* (Fig. 4G), both Permian in age, contain complex variations on the theme seen in earlier Carboniferous medullosans (Rössler, 2006).

Fortunately, medullosan whole-plant architecture can be understood to a moderate degree of accuracy. The complexity of medullosan fronds (Fig. 5A), when combined with reasonable measurements of individual pinnule area, can yield a photosynthetic surface area of more than two meters per frond, and perhaps substantially greater—one reported frond was greater than 7 meters in length (Laveine, 1986). Although it is impossible to know for certain how many leaves were active on any



FIGURE 4.—Examples of leaves and stems of a variety of medullosan taxa. A) Compression of *Alethopteris* pinnule (Harvard University Paleobotanical Collection; HUPC), interpreted as slower-growing, longer-lived leaves, from a mire-occupying medullosan (Raymond et al. 2014). B) Compression of a *Neuropteris* pinna from the Mazon Creek Formation (IL); HUPC. Interpreted as foliage of a faster-growing, shorter-lived, streamside medullosan. C) *Medullosa anglica* (HUPC #7791). D) Medullosan stem with large cortical tissues, preserved in coal ball material from Iowa. See Wilson and Fischer (2011) for details. E) *Colpoxylon*, a Permian medullosan. Specimen courtesy of Jean Galtier. F) *Medullosa stellata*, a Permian medullosan. Specimen courtesy of Jean Galtier.

FIGURE 5.—Morphology and interpretation of medullosan architecture. A) Reconstruction of a typical medullosan frond (form genus *Laveineopteris*), modified from Laveine (1997). Note that each frond contains several orders of pinnae, which combine to yield a massive leaf area. Based on observations of petiole length (Wnuk and Pfefferkorn 1984), medullosan fronds often exceeded 2 meters in length, and could reach up to 7 m in length. B) Medullosan stem preserved with branching order intact, described in and reproduced from Sterzel (1918), likely Permian in age from Germany (specimen destroyed in World War II). Based on this fossil, medullosan stems were capable of supporting several independently functioning fronds at the same time. See Pfefferkorn et al. (1984) for further discussion. C) Cross-section of permineralized pinnule of *Alethopteris lesquereauxii*, described by Raymond et al. (2014). Note the thin size of the leaf. Scale bar = 1mm. Reprinted from *Review of Palaeobotany and Palynology* v. 200, Raymond et al., “Permineralized *Alethopteris ambigua* (Lesquereux) White: A medullosan with relatively long-lived leaves, adapted for sunny habitats in mires and floodplains,” p. 82–96, © 2014 with permission of Elsevier. ⇒

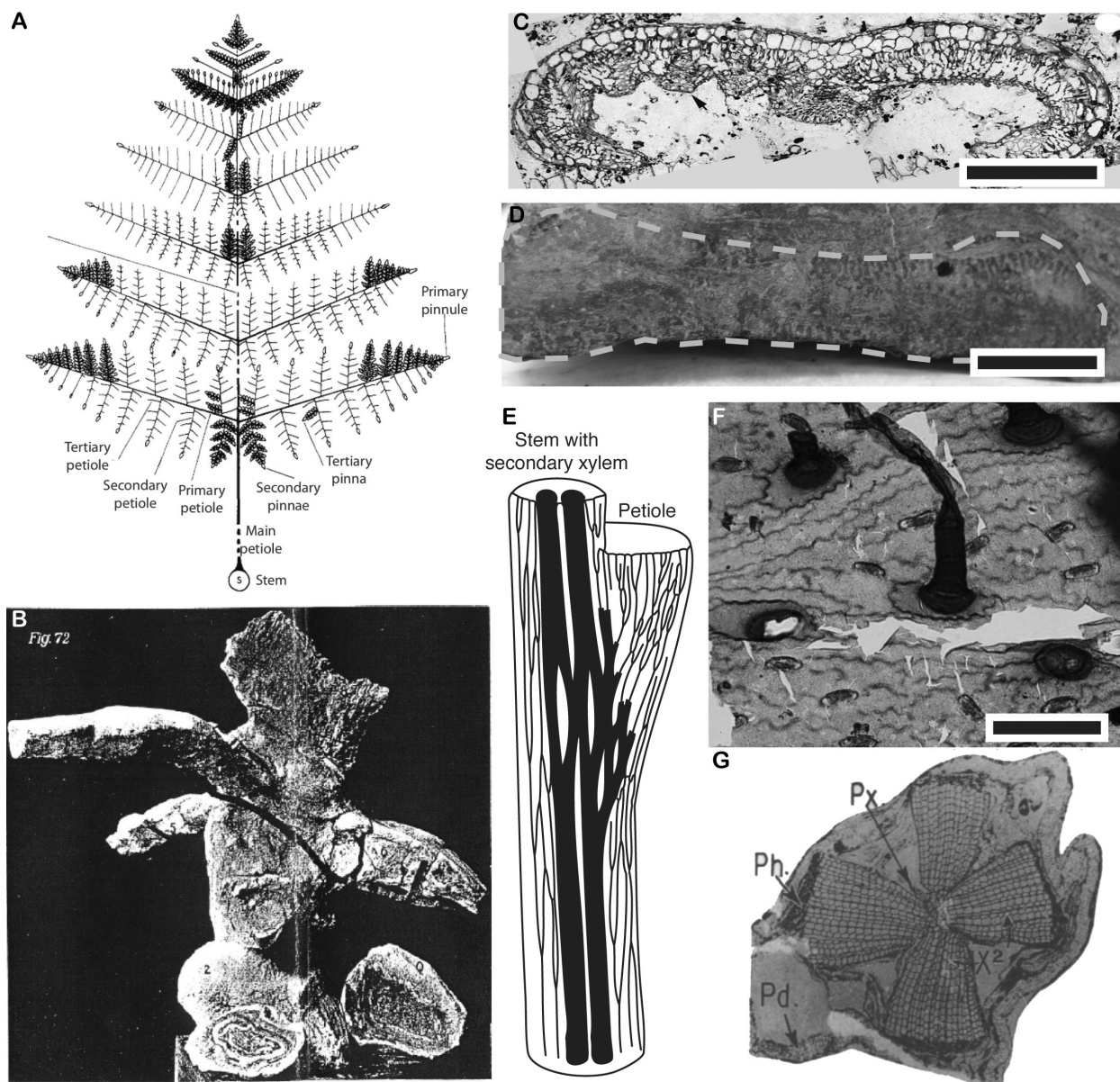


FIGURE 5. *cont. from previous page*—D) Cross-section of a medullosan branch, assigned to the form genus *Myeloxylon*. External tissues can be identified in coal-ball material because of their distinctive stippled texture. Scale bar = 1cm. E) Diagram of the vascular system of *Medullosa heterostelica* from West Mineral, KS, based on Stewart and Delevoryas (1952). Solid black areas are vascular segments (primary and secondary xylem; the stele); lines are leaf traces. Note anastomosing nature of the medullosan vascular system. F) Photomicrograph of an isolated medullosan cuticle from the Danville Coal (UC-Davis ID: FN111-40B1d). Note stomatal size and preserved trichomes. Scale bar = ~100 μm. G) Cross-section of medullosan root, modified from Steidtmann (1944). Note the tetrarch arrangement of xylem. (Px = protoxylem; Ph = phloem; Pd = root periderm). Reprinted with permission of the University of Michigan Museum of Paleontology.

individual extinct plant at a given time, a remarkable fossil that was described by Sterzel in 1918 captures the top of a Permian medullosan plant with several “branches” (leaf bases) attached, suggesting that medullosans were capable of supporting several actively photosynthesizing fronds at the same time

(Sterzel, 1918; Fig. 5B). Such an architecture implies that there were several large fronds active on any individual medullosan at the same, which could yield a leaf area of tens of square meters per stem. When the internal anatomy of the leaves is preserved, both *Alethopteris* and *Neuropteris* pinnules are relatively thin, with large stomata

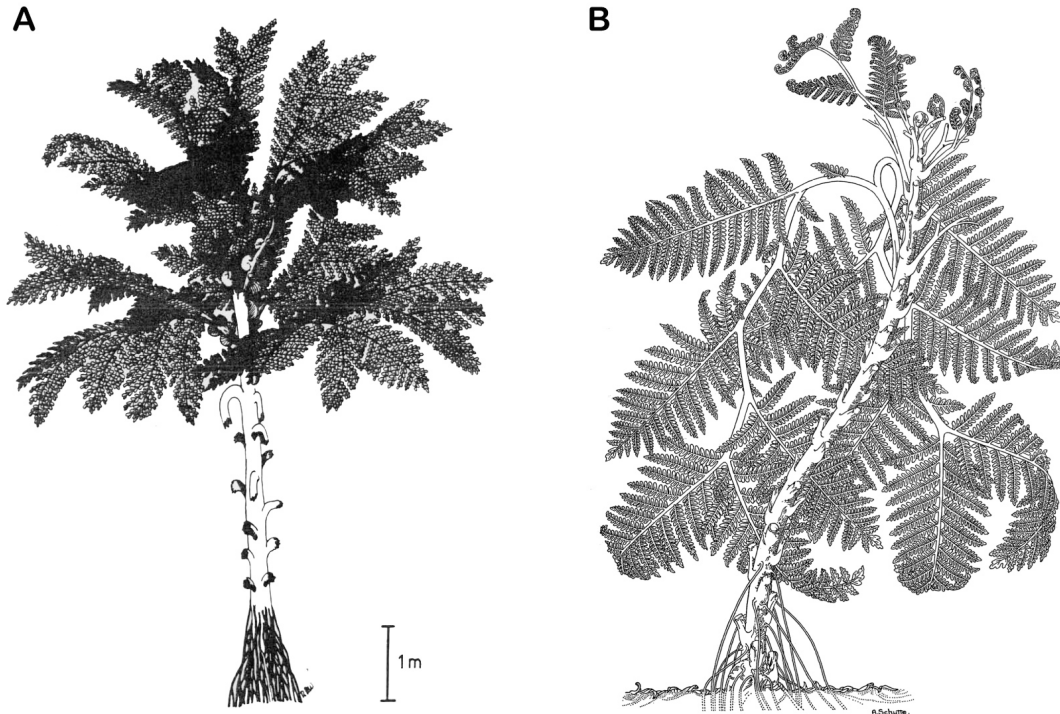


FIGURE 6.—Whole-plant reconstructions of *Medullosa* species depicting the overall architecture of a medullosan plant. A) Reconstruction of an erect medullosan based on compression fossils from Pennsylvania described by Wnuk and Pfefferkorn (1984) and explicated by Pfefferkorn et al. (1984). This reconstruction is drawn as if a medullosan leaf system was entire-margined to simplify the overall architecture, but in reality, each frond was a large compound system. Note persistent leaf bases on the stem. Reprinted with permission of the Delaware Valley Paleontological Society. B) Reconstruction of a lax-stemmed medullosan, *Medullosa thompsonii*, from Andrews and Kernen (1946). Note that the branches and leaves are drawn as if the plant were wilting in order to fit on a journal page. In life, they were likely held erect. Reprinted with permission from the Missouri Botanical Garden Press.

and veins in close proximity to sites of evaporation (Fig. 5C), and isolated medullosan cuticle preserves not only stomata, but, occasionally, epidermal trichomes—hairs adapted for either climbing or defense (Fig. 5F). The peripheral regions of medullosan petioles contained a set of cortical tissues that are widespread in coal ball material (Fig. 5D). The internal anatomy of medullosan petioles and rachises (assigned to the form genus *Myeloxylon*) is characterized by an abundance of ground tissue with several dozen individual leaf traces scattered throughout, each containing several xylem cells and rarely preserved phloem cells. Rare finds have permitted certain types of medullosan foliage to be confidently associated with individual stem anatomical types (Beeler, 1983; Pryor, 1990; Stull et al., 2012), and work on medullosan roots (Steidtmann, 1944; Rothwell and Whiteside, 1974; Fig. 5G) has allowed the whole plant to be reconstructed from roots to leaves. A number of detailed reconstructions have

been made of free-standing (Fig. 6A), leaning (Fig. 6B), or climbing liana and vine-like medullosans.

Summary of *Medullosa*

As a whole plant, the typical Carboniferous medullosan can be characterized as a small- to medium-sized tree, leaning tree, vine, or liana, bearing large fronds and supported by a relatively simple rooting system, with triarch, tetrarch, or pentarch roots developing adventitiously from the base of the stem. The anatomy of the stem indicates a large amount of stem cross-sectional area devoted to xylem, creating a large water-transport system. The individual water-conducting cells of the xylem, both primary and secondary, are among the largest diameter known from any late Paleozoic plant (100 to >250 μm in diameter), and are as large, or larger, than vessel elements in most angiosperms (Andrews and Kernen, 1946; Cichan, 1986; Wilson et al., 2008). The vascular system of the fronds was likewise

well-supplied with water-transport tissues. The fronds varied from ~1 m up to 7 m in length, and were highly divided in a pinnate manner. Individual pinnules were numerous, had high vein densities (2.5–5.5 mm mm⁻²; Boyce and Zwienecke, 2012) relative to other Pennsylvanian plants (< 3 mm mm⁻²; Boyce and Zwienecke, 2012), relatively thin laminae, and abundant, large, stomata, which would have facilitated water movement to and through the leaves. The exact number of functional leaves at any given time is not known for any medullosan species, but umbrella-like crowns have been assumed.

Ecophysiological assessment of medullosans

Hydraulic conductivity within medullosan pteridosperms must have been extremely high. The large diameters and extreme lengths of individual tracheary elements permit individual stem tracheids to approach hydraulic conductivity ranges found within angiosperm vessels, even when using conservative values for the porosity of individual pit membranes, reducing the overall conductivity of a medullosan tracheid (Wilson et al., 2008). These results are consistent with calculations made using only the diameter of individual cells and not taking pit structure into account (Cichan, 1986) and qualitative predictions made from anatomy alone (Andrews and Mamay, 1953). Previously published work has shown that individual medullosan tracheids have been modeled to possess a conduit-specific conductivity of 0.2 to 2.0 m² MPa⁻¹ s⁻¹ (Wilson et al., 2008; Wilson and Knoll, 2010), comparable to values measured from angiosperm vessels, which can possess a range of conduit-specific conductivities from 0.1 to more than 2.0 m² MPa⁻¹ s⁻¹, depending on the vessel diameter and plant ecophysiology (Tyree and Zimmermann, 2002; Sperry et al., 2004).

When this range of values is applied to the typical medullosan stem cross-section, a range of stem hydraulic conductivity can be estimated. Using a conservative value for the amount of secondary xylem functioning when the plant was alive, 50%, suggests that even small medullosan stems (< 8 cm in diameter), which contained several hundred secondary xylem tracheids, were capable of supplying water to a crown area measured in the tens of square meters. Medullosan leaf xylem is relatively little-studied when compared with the stems, but measuring the vein to stomatal distance in a variety of medullosan leaves reveals the capacity for high

transpiration, even with relatively modest vein densities. Preliminary analysis of transverse sections of *Neuropteris ovata* leaves with preserved internal anatomy can yield distances as short as 200 to 250 μm, implying a very high K_{leaf} (~16 mmol H₂O m⁻² s⁻¹ MPa⁻¹; based on *N. ovata* (n=3) and *M. scheuchzeri* (n=3) from Steubenville, OH [Beeler, 1983]) and consequent theoretical maximal stomatal conductance to water.

Independent analyses of medullosan leaves support this conclusion. A mechanistic model of medullosan stomatal conductance to water, based on details of the medullosan stomatal aperture and stomatal frequency, is concordant with estimates of high transpiration ability derived from leaf cross-sections, also implying the capability for high transpiration when favorable environmental conditions permitted.

Preliminary analyses of maximum theoretical and operational stomatal conductance were made of two common medullosan leaf species from Pennsylvanian coal-ball deposits across North America: *Neuropteris ovata* and *Macroneuropteris scheuchzeri* (n = 53; unpublished data). By applying Equation 3 to stomatal density, pore length, and guard-cell width measurements made from fossil cuticle, a range of g_{wmax} values can be estimated from individual medullosan stomata (Fig. 7A). These estimates, when refined using a kernel density function to determine which g_{wmax} values occur with the highest frequency (and are therefore most representative of leaf g_{wmax}), show that both *Neuropteris ovata* and *Macroneuropteris scheuchzeri* had higher maximal stomatal conductances to water and higher operational stomatal conductances to water than extant gymnosperms, ferns, and many angiosperms. Maximal stomatal conductances to water estimated from the Calhoun Coal medullosans suggest ranges up to 3000 mmol H₂O m² s⁻¹. Taking a conservative approach to estimating the average operational stomatal conductance for one average case-study medullosan from the Calhoun Coal (*N. ovata* #38324) as 10% to 30% of g_{wmax} (McElwain et al., 2015 in press) yields ranges of 284–884 mmol H₂O m² s⁻¹ (Fig. 7B). These g_{op} values are comparable to those found in broadleaved angiosperms, including *Acer macrophyllum* (~260 mmol H₂O m² s⁻¹; Franks, 2004) and *Cornus nuttallii* (~350 mmol H₂O m² s⁻¹; Franks, 2004), and the medullosan g_{wmax} values are only surpassed by g_{wmax} values found

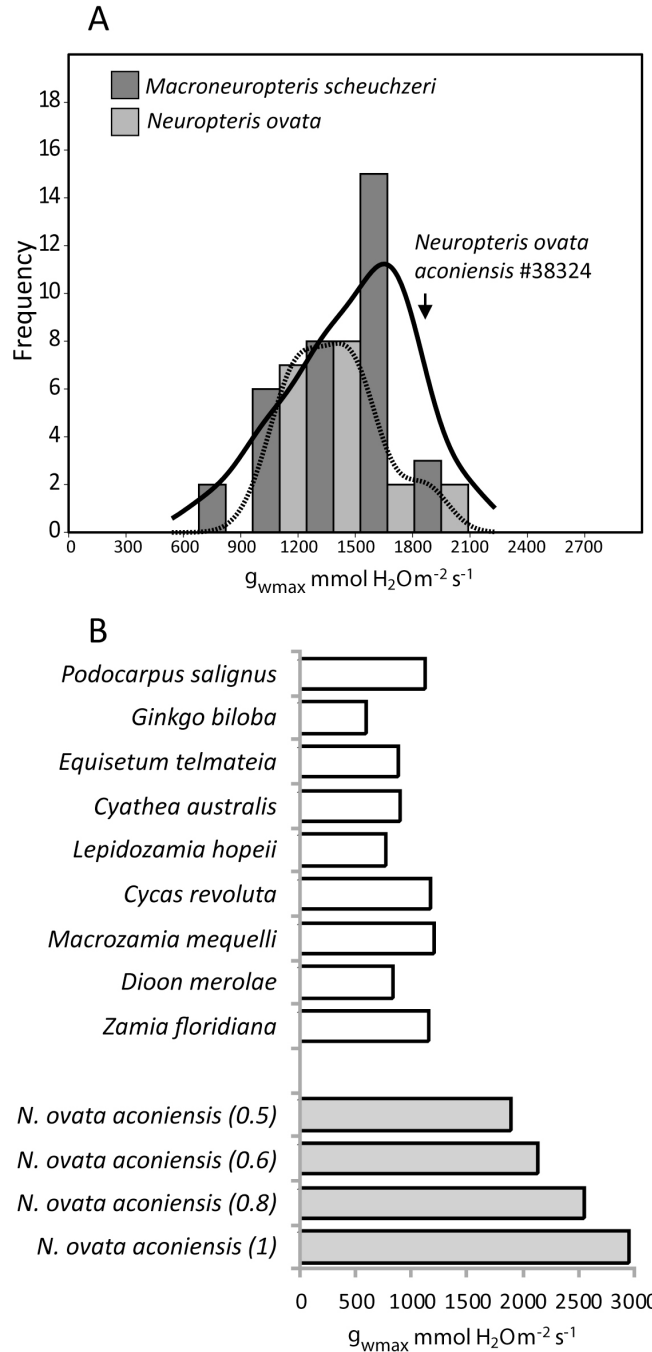


FIGURE 7.—A) Frequency distribution of G_{wmax} values calculated for *Neuropteris ovata* ($n=19$) and *Macroneuropteris scheuchzeri* ($n=34$) from Pennsylvanian coal deposits across North America. Lines are kernel density functions mapping the distribution of G_{wmax} values for each species. Arrow notes the modeled G_{wmax} of *Neuropteris ovata aconiensis* specimen #38324. B) G_{wmax} of *Neuropteris ovata aconiensis* (#38324) is compared with those of a range of extant gymnosperms (*Podocarpus salignus*, *Ginkgo biloba*, *Lepidozamia hopeii*, *Cycas revoluta*, *Macrozamia mequelli*, *Dioon merolae*, *Zamia floridiana*) and two monilophytes (*Equisetum telmateia*, *Cyathea australis*). G_{wmax} estimates for all extant taxa are based on the observation that stomata of gymnosperms and ferns open to 0.5 of a circle with a radius = ($1/2$ pore length) when fully open (Franks and Fraquhar, 2010). G_{wmax} values of *N. ovata aconiensis* are modeled based on different assumptions on the pore geometries when stomata are fully open including a circle (1) and 50% (0.5), 60% (0.6) and 80% (0.8) of a circle respectively. Based on other anatomical traits of the medullosans, including high-conductivity stem xylem and large leaf area, it is likely that medullosan stomata opened to a full circle, similar to modern angiosperms.

in tropical evergreen angiosperms. Further work will explore the variability in and among medullosan taxa through time, but the estimates of a high water vapor supply from large medullosan stomata is consistent with the ecophysiological interpretation derived from medullosan xylem and leaf size: these were plants with anatomical structures capable of supporting a high transpiration rate and must have driven a large evapotranspirative flux.

DISCUSSION

Plant architecture

The medullosans were a highly diverse, architecturally variable group of plants (e.g. Pfefferkorn et al., 1984); some were self-supporting, whereas others appear to have been tall “leaners” that formed thickets (Wnuk and Pfefferkorn, 1984), and others were lianas (Hamer and Rothwell, 1988; Dunn et al., 2003) or low canopy plants in areas where large trees were lacking (Gastaldo et al., 2004; Opluštil et al., 2009). Thus, it is difficult to make general statements about the details of water-transport physiology that can be applied without qualification to all of the many genera and species. Nonetheless, based on anatomical studies, medullosans shared the characteristics of large frond size, relatively thin foliage with relatively high vein densities in comparison to other Carboniferous plants, and vasculature in the stem and leaf capable of transporting high volumes of water. Thus, as a group, the kind of water-conducting capacity estimated here was probably relatively widespread within the clade. As a first attempt at such an estimate, data indicate that the medullosans were distinctively different from all other groups of plants that made significant contributions to Pennsylvanian wetland biomass.

The medullosans were most abundant in wetlands or in perihumid conditions. Thus, they were common in Pennsylvanian coal-swamp settings (Phillips et al., 1985) at all times, unlike (e.g.) the tree ferns, which rose to prominence in the later Middle Pennsylvanian through Upper Pennsylvanian, or the lycopsids, which declined steeply in the Upper Pennsylvanian, and were among the most abundant plants in mineral soil wetlands during this same time interval (e.g., Pfefferkorn and Thomson, 1982). Consequently, the contribution of their hydraulic output was a considerable part of the dynamic water-use

patterns and efficiency of a Pennsylvanian-age, tropical wetland forest.

The climatic influence of the medullosans, and specifically their high hydraulic output, is interesting to consider. There is a rich literature on the influence of modern tropical rainforests on regional and global climate, motivated largely by the current deforestation and fragmentation of the rainforests for anthropogenic purposes. Modern tropical rainforests are known to efficiently recycle water, to the extent that about one-half of the moisture used for precipitation is supplied through local evapotranspiration (Salati, 1987). Evapotranspiration increases boundary layer moisture and, at the same time, decreases moisture convergence over rain forests (Lee et al., 2012), reducing intra-seasonal precipitation variability. The large evapotranspiration flux from rainforests generally results locally in slight surface cooling and an increase in both cloud cover and precipitation (e.g., Lawrence and Vadecar, 2015). As a source of latent heat, evapotranspiration fluxes can cause atmospheric instability and trigger convection. However, it is not clear from the literature whether rainforests result in more frequent or intense convection than deforested areas. Rainforests also affect remote extratropical regions through atmospheric teleconnections. Perturbations to rainforests in climate models can cause remote drying or precipitation increases (Werth and Avissar, 2002; Nobre et al., 2009).

A medullosan-dominated forest is likely to represent a modern tropical rainforest evapotranspiration in overdrive. Large evapotranspiration fluxes would have caused local tropical cooling, an increase in cloud cover and precipitation, and reduced intra-seasonal precipitation variability. Remote effects are difficult to predict without use of a climate model, but it is quite likely that tropical-extratropical moisture transport would have been enhanced, leading to regions of higher aridity or greater rainfall. A final consideration is that the range of medullosan-dominated forests was likely dynamic. Paleoclimate simulations of the late Paleozoic indicate that the distribution of tropical forest biomes may have responded to glacial-interglacial changes, atmospheric CO₂, and orbital variations (Poulsen et al., 2007; Horton et al., 2012). Climate-induced expansion and retraction of medullosan-dominated forested areas would have caused further variability of the late Paleozoic hydrologic cycling.

FRONTIERS—THE WAY FORWARD

The late Paleozoic icehouse witnessed the evolution and expansion of the oldest and most extensive paleotropical forests (Cleal and Thomas, 2005), for which the vegetation is among the best studied and most fully known of the Phanerozoic history of terrestrial plants. Within this climatically dynamic icehouse, shifts in the composition of paleotropical flora in step with glacial and interglacial states of eccentricity-paced cycles (Falcon-Lang, 2003; 2004; Falcon-Lang et al., 2006; 2009; Falcon-Lang and DiMichele, 2010, DiMichele et al., 2010) and between 10^6 yr-scale discrete glaciations and intermittent glacial minima (Gastaldo et al., 1996; Montañez et al., 2007; Plotnick et al., 2009; Tabor et al., 2013) have been well documented. Within the longer-term changes were abrupt periods (Atokan-Desmoinesian, Middle to Upper Pennsylvanian, and Permo-Carboniferous boundaries) of major intra- and inter-biomic reorganization of dominance and diversity in tropical lowland vegetation (DiMichele et al., 2006, 2008; van Hoof et al., 2013). Each of these events was marked by substantial change in climate and likely ice volume and at least one event, the Middle–Upper Pennsylvanian boundary, exhibited ecological threshold behavior (Pfefferkorn et al., 2008; DiMichele et al., 2009). These reconstructed climate-vegetation relationships have facilitated the recognition of distinct Pennsylvanian biomes, and suggest the existence of strong linkages between climate and terrestrial vegetation.

Modeling studies of modern and future climate reveal that physiological responses of terrestrial vegetation to increasing CO_2 and/or water stress can influence regional surface temperatures, water cycling, atmospheric circulation, and terrestrial C sequestration, which can translate to much broader-scale changes in climate, continental runoff, and atmospheric greenhouse-gas concentrations (Sellers et al., 1996; DeFries et al., 2002; Feddema et al., 2005; Gedney et al., 2006; Betts et al., 2007; Nugent and Matthews, 2012). This ELT collaborative research is driven by the hypothesis that large variability in leaf conductance and whole-plant hydraulic capacity among different groups of late Paleozoic vegetation, including the recently revealed evapotranspiration potential of the medullosan-dominated forests comparable to angiosperms, when coupled with temporal

changes in floral composition in the tropical lowlands, may have contributed to substantial differences in physiological forcing of the hydrological cycle during glacial-interglacial climate states of the late Paleozoic icehouse. Furthermore, phenotypically plastic developmental changes in stomatal traits in response to changes in atmospheric CO_2 and/or water stress have been documented by experimental studies (Ainsworth and Long, 2005; Berry et al., 2010; Lammertsma et al., 2011) and verified using herbarium and fossil plant analysis (Wagner et al., 2005). This physiological response at the leaf scale can translate to large changes in canopy-scale transpiration rates through time if unaccompanied by structural responses, such as enhanced leaf growth and consequent increased surface area for transpiration (i.e., increased leaf-area index; Steinhorsdottir et al., 2012). In turn, changes in canopy-scale transpiration rates influence regional climate and surface runoff on a regional- to continental-scale (Betts et al., 2007; Boyce and Lee, 2010; Berry et al., 2010; de Boer et al., 2011). Continued study of the fossil plant dominants in the wetland and seasonally dryland floras of the Pangaeian tropical lowlands should reveal evidence for such variability in physiological responses across the landscape and through time, given the magnitude of previously reconstructed climate changes for the late Paleozoic icehouse (summarized in Montañez and Poulsen, 2013).

Plant adaptation to environmental forcing and scaling to ecosystem response is complex, involving the interplay of many biological and environmental conditions. To evaluate physiological forcing of late Paleozoic tropical climate will require a more thorough characterization of the natural variability in whole-plant traits within and between representative taxa of the different species pools, an understanding of how these traits map onto physiological function, and a quantitative evaluation of how tropical vegetation may have responded to environmental forcing under conditions representative of the Late Paleozoic Ice Age (LPIA). These issues are being addressed using whole-plant reconstructions (where possible) of the dominant plants within the paleotropical species pools along with stable-isotope studies, and integrating these with experimental studies using plant material grown under controlled paleo-atmospheric conditions and ecosystem-scale modeling (BIOME-BGC)

parameterized for the LPIA low latitudes. Ultimately, these empirical and experimental results will be used to define plant functional types for the Pangean paleotropics. These plant functional types will then be incorporated into a fully coupled Community Earth-System Model, which will investigate the potential of climate-CO₂-vegetation feedbacks to push the late Paleozoic climate system between glacial and interglacial states, and to strongly modify the climate regime within these states.

CONCLUSIONS AND FINAL MESSAGES

Extant species are not always relevant to the study of extinct plants because they contain anatomy adapted to a long environmental and evolutionary history, and may not have analogous parts when compared to fossil plants. Plants have many parts, such as stems, roots, and leaves, but when plants are considered as entire organisms, their physiological properties can be clarified from optimal or maximum values to realistic or operating values. Contrary to the existing paradigm of the water-transport capacity of pre-angiosperm flora, a variety of modeling techniques applied to late Paleozoic medullosan stems and leaves indicate that their water-transport capabilities exceeded those found in living gymnosperms and many angiosperms.

The medullosans serve as an useful example of how the barriers to understanding Paleozoic plants' physiological properties are no different than those to reconstructing the physiology of (e.g.) Cretaceous angiosperms, assuming the laws of physics remain the same and despite anatomical and morphological differences between Paleozoic seed plants and living angiosperms. It is worth distinguishing between "familiar" plant forms and those that are "well-understood"—much more is known about medullosan plant architecture than that of some early angiosperms (e.g., *Sanmiguelia*). Fortunately for Earth scientists, through these Paleozoic plant fossils, important constraints on the late Paleozoic environment can begin to be derived.

ACKNOWLEDGMENTS

The authors would like to acknowledge NSF funding from the Earth-Life Transitions initiative (EAR-1338281 to IPM, JM and WD, EAR-1338256 to MH, EAR-1338247 to JDW,

and EAR-1338200 to CP), and the reviewers and editors of this issue for constructive comments.

REFERENCES

- Ainsworth, E. A., and S. P. Long. 2005. What have we learned from 15 years of free-air CO₂ enrichment (FACE)? A meta-analytic review of the responses of photosynthesis, canopy properties and plant reproduction to rising CO₂. *New Phytologist*, 165:351–372.
- Algeo, T. J., and S. E. Scheckler. 1998. Terrestrial-marine teleconnections in the Devonian: links between the evolution of land plants, weathering processes, and marine anoxic events. *Philosophical Transactions of the Royal Society B-Biological Sciences*, 353:113–128.
- Andrews, H. N., and J. A. Kernen. 1946. Contributions to our knowledge of American Carboniferous floras. VIII. Another *Medullosa* from Iowa. *Annals of the Missouri Botanical Garden*, 33:141–146.
- Andrews, H. N., and S. H. Mamay. 1953. Some American *Medullosas*. *Annals of the Missouri Botanical Garden*, 40: 183–209.
- Barthlott, W., and C. Neinhuis. 1997. Purity of the sacred lotus, or escape from contamination in biological surfaces. *Planta*, 202:1–8.
- Baas, P., R. Schmid, and B. J. Van Heuven. 1986. Wood anatomy of *Pinus longaeva* (Bristlecone Pine) and the sustained length-on-age increase of its tracheids. *IAWA Journal*, 7:221–228.
- Barbour, M. M. 2007. Stable oxygen isotope composition of plant tissue: a review. *Functional Plant Biology*, 34:83–94.
- Barbour, M. M., J. S. Roden, G. D. Farquhar, and J. R. Ehleringer. 2004. Expressing leaf water and cellulose oxygen isotope ratios as enrichment above source water reveals evidence of a Péclet effect. *Oecologia*, 138:426–435.
- Basinger, J. F., G. W. Rothwell, and W. N. Stewart. 1974. Cauline vasculature and leaf trace production in medullosan pteridosperms. *American Journal of Botany*, 61:1002–1015.
- Beeler, H. E. 1983. Anatomy and frond architecture of *Neuropteris ovata* and *Neuropteris scheuchzeri* from the upper Pennsylvanian of the Appalachian Basin. *Canadian Journal of Botany-Revue Canadienne De Botanique*, 61:2352–2368.
- Beerling, D. J., W. G. Chaloner, B. Huntley, J. A. Pearson, and M. J. Tooley. 1993. Stomatal density responds to the glacial cycle of environmental change. *Proceedings of the Royal Society B: Biological Sciences*, 251:133–138.
- Beerling, D. J., and W. G. Chaloner. 1993. Stomatal density as an indicator of atmospheric CO₂ concentration. *Holocene*, 2:71–78.
- Beerling, D. J., J. C. McElwain, and C. P. Osborne. 1998. Stomatal responses of the 'living fossil'

- Ginkgo biloba* L. to changes in atmospheric CO₂ concentrations: *Journal of Experimental Botany*, 49:1603–1607.
- Berry, J. A., D. J. Beerling, and P. J. Franks. 2010. Stomata: key players in the earth system, past and present. *Current Opinion in Plant Biology*, 13:233–240.
- Betts, R. A., O. Boucher, M. Collins, P. M. Cox, P. D. Falloon, N. Gedney, D. L. Hemming, C. Huntingford, C. D. Jones, D. M. H. Sexton, and M. J. Webb. 2007. Projected increase in continental runoff due to plant responses to increasing carbon dioxide. *Nature*, 448:1037–1041.
- Boyce, C. K., and A. H. Knoll. 2002. Evolution of developmental potential and the multiple independent origins of leaves in Paleozoic vascular plants. *Paleobiology*, 28:70–100.
- Boyce, C. K., T. J. Brodrigg, T. S. Feild, and M.A. Zwieniecki. 2009. Angiosperm leaf vein evolution was physiologically and environmentally transformative. *Proceedings of the Royal Society B: Biological Sciences*, 276:1771–1776.
- Boyce, C. K., J. E. Lee, T. S. Feild, T. J. Brodrigg, and M. A. Zwieniecki. 2010. Angiosperms helped put the rain in the rainforests: the impact of plant physiological evolution on tropical biodiversity. *Annals of the Missouri Botanical Garden*, 97:527–540.
- Boyce, C. K., and Lee, J-E. 2010. An exceptional role for flowering plant physiology in the expansion of tropical rainforests and biodiversity. *Proceedings of the Royal Society B: Biological Sciences*, doi: 10.1098/rspb.2010.0485.
- Brongniart, A. 1828. *Prodrome d'une Histoire des Végétaux Fossiles*. Grand Dictionnaire d'Histoire Naturelle, Paris, F. G. Levrault, 57:170–212.
- Brodersen, C., S. Jansen, B. Choat, C. Rico, and J. Pittermann. 2014. Cavitation resistance in seedless vascular plants: The structure and function of interconduit pit membranes. *Plant Physiology*, 165:895–904.
- Brodersen, C. R., and A. J. McElrone. 2013. Maintenance of xylem network transport capacity: A review of embolism repair in vascular plants. *Frontiers in Plant Science*, 4:108.
- Brodersen, C. R., A. J. McElrone, B. Choat, M. A. Matthews, and K. A. Shackel. 2010. The dynamics of embolism repair in xylem: In vivo visualizations using high-resolution computed tomography. *Plant Physiology*, 154:1088–1095.
- Brodrigg, T. J., T. S. Feild, and G. J. Jordan. 2007. Leaf maximum photosynthetic rate and venation are linked by hydraulics. *Plant Physiology*, 144:1890–1898.
- Canadell, J., R. B. Jackson, J. R. Ehleringer, H. A. Mooney, O. E. Sala, E.-D. Schulze. 1996. Maximum rooting depth of vegetation types at the global scale. *Oecologia*, 108:583–595.
- Casson, S. A., and A. M. Hetherington. 2010. Environmental regulation of stomatal development. *Current Opinion in Plant Biology*, 13:90–95.
- Cernusak, L. A., K. Winter, J. Aranda, and B. L. Turner. 2008. Conifers, angiosperm trees, and lianas: growth, whole-plant water and nitrogen use efficiency, and stable isotope composition ($\delta^{13}\text{C}$ and $\delta^{18}\text{O}$) of seedlings grown in a tropical environment. *Plant Physiology*, 148:642–659.
- Cichan, M. A. 1986. Conductance in the wood of selected Carboniferous plants. *Paleobiology*, 12:302–310.
- Cichan, M. A., and T. N. Taylor. 1984. A method for determining tracheid lengths in petrified wood by analysis of cross-sections. *Annals of Botany*, 53:219–226.
- Choat, B., M. Ball, J. Lully, and J. Holtum. 2003. Pit membrane porosity and water stress-induced cavitation in four co-existing dry rainforest tree species. *Plant Physiology*, 131:41–48.
- Choat, B., T. W. Brodie, A. R. Cobb, M. A. Zwieniecki, and N. M. Holbrook. 2006. Direct measurements of intervessel pit membrane hydraulic resistance in two angiosperm tree species. *American Journal of Botany*, 93:993–1000.
- Choat, B., A. R. Cobb, and S. Jansen. 2008. Structure and function of bordered pits: new discoveries and impacts on whole-plant hydraulic function. *New Phytologist*, 177:608–626.
- Clearwater, M. J., and C. J. Clark. 2003. In vivo magnetic resonance imaging of xylem vessel contents in woody lianas. *Plant, Cell and Environment*, 26:1205–1214.
- Cleal, C. J., and C. H. Shute. 2003. Systematics of the late Carboniferous medullosalean pteridosperm *Laveineopteris* and its associated *Cyclopteris* leaves. *Palaeontology*, 46:353–411.
- Cleal, C. J., C. H. Shute, and E. L. Zodrow, E.L. 1990. A revised taxonomy for Palaeozoic neuropterid foliage. *Taxon*, 39:486–492.
- Cleal, C. J., and B. A. Thomas. 2005. Palaeozoic tropical rainforests and their effect on global climates: Is the past the key to the present? *Geobiology*, 3:13–31.
- Comstock, J. P., and J. S. Sperry. 2000. Theoretical considerations of optimal conduit length for water transport in vascular plants. *New Phytologist*, 148:195–218.
- Craig, H., and Gordon, L. I. 1965. Deuterium and oxygen-18 variations in the ocean and the marine atmosphere, p. 9–130. *In* E. Tongiorgi (ed.), *Proceedings of a Conference on Stable Isotopes in Oceanographic Studies and Paleotemperatures*. Spoleto, Italy.
- Crane, P. R. 1985. Phylogenetic analysis of seed plants and the origin of angiosperms. *Annals of the*

- Missouri Botanical Garden, 72:716–793.
- Damour, G., T. Simonneau, H. Cochard, and L. Urban. 2010. An overview of models of stomatal conductance at the leaf level. *Plant, Cell and Environment*, 33:1419–1438.
- Dawson, T. E., S. Mambelli, A. H. Plamboeck, P. H. Templer, and K. P. Tu. 2002. Stable isotopes in plant ecology. *Annual Review of Ecology and Systematics*, 33:507–559.
- De Boer, H. J., E. I. Lammertsma, F. Wagner-Cremer, D. L. Dilcher, M. J. Wassen, and S. C. Dekker. 2011. Climate forcing due to optimization of maximal leaf conductance in subtropical vegetation under rising CO₂. *Proceedings of the National Academy of Sciences*, 108:4041–4046.
- Defries, R. S., R. A. Houghton, M. C. Hansen, C. B. Field, D. Skole, and J. Townshend. 2002. Carbon emissions from tropical deforestation and regrowth based on satellite observations for the 1980s and 1990s. *Proceedings of the National Academy of Sciences*, 99:14256–14261.
- Delevoryas, T. 1955. The Medullosae: structure and relationships. *Palaeontographica B*, 97:114–167.
- Dennis, R. L., and D. A. Eggert. 1978. *Parasporotheca* gen. nov., and its bearing on interpretation of morphology of permineralized medullosan pollen organs. *Botanical Gazette*, 139:117–139.
- DiMichele, W. A., B. Cecil, I. P. Montañez, and H. Falcon-Lang. 2010. Cyclic changes in Pennsylvanian paleoclimate and effects on floristic dynamics in tropical Pangaea. *International Journal of Coal Geology*, 83:329–344.
- DiMichele, W. A., H. Kerp, N. J. Tabor, and C. V. Looy. 2008. Revisiting the so-called “Paleophytic-Mesophytic” transition in equatorial Pangea: vegetational integrity and climatic tracking. *Palaeogeography, Palaeoclimatology, Palaeoecology*, 268:152–163.
- DiMichele, W. A., I. P. Montañez, C. J. Poulsen, and N. J. Tabor. 2009. Vegetation-climate feedbacks and regime shifts in the Late Paleozoic ice age earth. *Geobiology*, 7:200–226.
- DiMichele, W. A., N. J. Tabor, D. S. Chaney, and W. J. Nelson. 2006. From wetlands to wetspots: the fate and significance of Carboniferous elements in early Permian coastal plain floras of north-central Texas, p. 223–248. *In* S. Greb and W. A. DiMichele (eds.), *Wetlands Through Time*. Geological Society of America Special Publications 299, Boulder, CO.
- Dow, G. J., D. C. Bergmann, and J. A. Berry. 2014. An integrated model of stomatal development and leaf physiology. *New Phytologist*, 201:1218–1226.
- Doyle, J. A. 2006. Seed ferns and the origin of angiosperms. *Journal of the Torrey Botanical Society*, 133:169–209.
- Drinnan, A. N., and P. R. Crane. 1994. A synopsis of medullosan pollen organs from the middle Pennsylvanian Mazon-Creek Flora of northeastern Illinois, USA. *Review of Palaeobotany and Palynology*, 80:235–257.
- Dunn, M. T. 2006. A review of permineralized seed fern stems of the Upper Paleozoic. *Journal of the Torrey Botanical Society*, 133:20–32.
- Dunn, M. T., M. Krings, G. Mapes, G. W. Rothwell, R. H. Mapes, and S. Keqin. 2003. *Medullosa steinii* sp. nov., a seed fern vine from the upper Mississippian. *Review of Palaeobotany and Palynology*, 124:307–324.
- Edwards, D., H. Kerp, and H. Hass. 1998. Stomata in early land plants: an anatomical and ecophysiological approach. *Journal of Experimental Botany*, 49:255–278.
- Eggert, D. A., and G. W. Rothwell. 1979. *Stewartiothea* gen. n. and the nature and origin of complex permineralized medullosan pollen organs. *American Journal of Botany*, 66:851–866.
- Falcon-Lang, H. J. 2003. Response of Late Carboniferous tropical vegetation to transgressive–regressive rhythms at Joggins, Nova Scotia. *Journal of the Geological Society of London*, 160:643–648.
- Falcon-Lang, H. J. 2004. Pennsylvanian tropical rain forests responded to glacial-interglacial rhythms. *Geology*, 32:689–692.
- Falcon-Lang, H. J., M. J. Benton, S. J. Braddy, and S. J. Davies. 2006. The Pennsylvanian tropical biome reconstructed from the Joggins Formation of Nova Scotia, Canada. *Journal of the Geological Society of London*, 163:561–576.
- Falcon-Lang, H. J., and W. A. DiMichele. 2010. What happened to the coal forests during Pennsylvanian glacial phases? *Palaios*, 25:611–617.
- Falcon-Lang, H. J., W. J. Nelson, S. Elrick, C. V. Looy, P. R. Ames, and W. A. DiMichele. 2009. Incised channel-fills containing conifers indicate that seasonally dry vegetation dominated Pennsylvanian tropical lowlands. *Geology*, 37:923–926.
- Farquhar, G. D., L. A. Cernusak, and B. Barnes. 2007. Heavy water fractionation during transpiration. *Plant Physiology*, 143:11–18.
- Farquhar, G. D., J. R. Ehleringer, and K. T. Hubick. 1989a. Carbon isotope discrimination and photosynthesis. *Annual Review of Plant Physiology and Plant Molecular Biology*, 40:503–537.
- Farquhar, G. D., K. T. Hubick, A. G. Condon, and R. A. Richards. 1989b. Carbon isotope fractionation and plant water-use efficiency, p. 21–40. *In* P. W. Rundel, J. R. Ehleringer, and K. A. Nagy (eds.), *Stable Isotopes in Ecological Research*. Springer-Verlag, New York.
- Farquhar, G. D., M. H. O’Leary, and J. A. Berry. 1982. On the relationship between carbon isotope discrimination and the intercellular carbon dioxide

- concentration in leaves. *Australian Journal of Plant Physiology*, 9:121–137.
- Farquhar, G. D., and T. D. Sharkey. 1982. Stomatal conductance and photosynthesis. *Annual Review of Plant Physiology*, 33:317–345.
- Feddema, J. J., K. W. Oleson, G. B. Bonan, L. O. Mearns, L. E. Buja, G. A. Meehl, and W. M. Washington. 2005. The importance of land-cover change in simulating future climates. *Science*, 310:1674–1678.
- Feild, T. S., T. J. Brodribb, A. Iglesias, D. S. Chatelet, A. Baresch, G. R. Upchurch, B. Gomez, B. A. R. Mohr, C. Coiffard, J. Kvacek, and C. Jaramillo. 2011. Fossil evidence for Cretaceous escalation in angiosperm leaf vein evolution. *Proceedings of the National Academy of Sciences*, 108:8363–8366.
- Fielding, C. R., T. D. Frank, and J. L. Isbell (eds.). 2008. *Resolving the Late Paleozoic Ice Age in Time and Space*. Geological Society of America Special Publications 441. Boulder, CO.
- Flanagan, L. B., J. P. Comstock, and J. R. Ehleringer. 1991. Comparison of modeled and observed environmental influences on the stable oxygen and hydrogen isotope composition of leaf water in *Phaseolus vulgaris* L. *Plant Physiology*, 96:588–596.
- Flanagan, L. B., and J. R. Ehleringer. 1991. Effects of mild water stress and diurnal changes in temperature and humidity on the stable oxygen and hydrogen isotopic composition of leaf water in *Cornus stolonifera* L. *Plant Physiology*, 97:298–305.
- Franks, P. J. 2004. Stomatal control and hydraulic conductance, with special reference to tall trees. *Tree Physiology*, 24:865–878.
- Franks, P. J., D. L. Royer, D. J. Beerling, P. K. van de Water, D. J. Cantrill, M. M. Barbour, and J. A. Berry. 2014. New constraints on atmospheric CO₂ concentration for the Phanerozoic. *Geophysical Research Letters*, 41:4685–4694.
- Galtier, J. 1988. Morphology and phylogenetic relationships of early pteridosperms, p. 135–176. *In* C. Beck (ed.), *Origin and Evolution of Gymnosperms*: Columbia University Press, New York.
- Gastaldo, R. A., I. M. Stevanović-Walls, W. N. Ware, and S. F. Greb. 2004. Community heterogeneity of Early Pennsylvanian peat mires. *Geology*, 32:693–696.
- Gastaldo, R. A., W. A. DiMichele, and H. W. Pfefferkorn. 1996. Out of the icehouse into the greenhouse: a Late Paleozoic analog for modern global vegetational change. *GSA Today*, 6:1–7.
- Gedney, N., P. M. Cox, R. A. Betts, O. Boucher, C. Huntingford, and P. A. Scott. 2006. Detection of a direct carbon dioxide effect in continental river runoff records. *Nature*, 439:853–858.
- Gleason, S. M., C. J. Blackman, A. M. Cook, C. A. Laws, and M. Estoby. 2014. Whole-plant capacitance, embolism resistance and slow transpiration rates all contribute to longer desiccation times in woody angiosperms from arid and wet habitats. *Tree Physiology*, 34:275–284.
- Grams, T. E., A. R. Kozovits, K. H. Haberle, R. Matyssek, and T. E. Dawson. 2007. Combining $\delta^{13}\text{C}$ and $\delta^{18}\text{O}$ analyses to unravel competition, CO₂ and O₃ effects on the physiological performance of different-aged trees. *Plant Cell and Environment*, 30:1023–1034.
- Hacke, U. G., and J. S. Sperry. 2001. Functional and ecological xylem anatomy. *Perspectives in Plant Ecology Evolution and Systematics*, 4:97–115.
- Hacke, U. G., and J. S. Sperry. 2003. Limits to xylem refilling under negative pressure in *Laurus nobilis* and *Acer negundo*. *Plant Cell and Environment*, 26:303–311.
- Hacke, U. G., J. S. Sperry, and J. Pittermann. 2000. Drought experience and cavitation resistance in six shrubs from the Great Basin, Utah. *Basic and Applied Ecology*, 1:31–41.
- Hacke, U. G., J. S. Sperry, and J. Pittermann. 2004. Analysis of circular bordered pit function—II. Gymnosperm tracheids with torus-margo pit membranes. *American Journal of Botany*, 91:386–400.
- Hacke, U. G., J. S. Sperry, J. K. Wheeler, and L. Castro. 2006. Scaling of angiosperm xylem structure with safety and efficiency. *Tree Physiology*, 26:689–701.
- Hacke, U. G., V. Stiller, J. S. Sperry, J. Pittermann, and K. A. McCulloh. 2001. Cavitation fatigue. Embolism and refilling cycles can weaken the cavitation resistance of xylem. *Plant Physiology*, 125:779–786.
- Hamer, J. J., and G. W. Rothwell. 1988. The vegetative structure of *Medullosa endocentrica* (Pteridospermopsida). *Canadian Journal of Botany-Revue Canadienne De Botanique*, 66:375–387.
- Haworth, M., C. Elliott-Kingston, J. C. McElwain. 2013. Co-ordination of physiological and morphological responses of stomata to elevated [CO₂] in vascular plants. *Oecologia*, 171:71–82.
- Hetherington, A. M., and F. I. Woodward. 2003. The role of stomata in sensing and driving environmental change. *Nature*, 424:901–908.
- Hilton, J., and R. M. Bateman. 2006. Pteridosperms are the backbone of seed-plant phylogeny. *Journal of the Torrey Botanical Society*, 133:119–168.
- Holloway, J. P. 1969. The effects of superficial wax on leaf wettability. *Annals of Applied Biology*, 63:145–153.
- Horton, D. E., C. J. Poulsen, I. P. Montañez, and W. A. Dimichele. 2012. Eccentricity-paced late Paleozoic climate change. *Palaeogeography, Palaeoclimatology, Palaeoecology*, 331–332:150–

- 161.
- Hren, M. T., M. Pagani, and M. Brandon. 2010. Biomarker reconstruction of the early Eocene paleotopography and paleoclimate of the northern Sierra Nevada. *Geology*, 38:7–10.
- Jansen, S., B. Choat, and A. Pletsers. 2009. Morphological variation of intervessel pit membranes and implications to xylem function in angiosperms. *American Journal of Botany*, 96:409–419.
- Keitel, C., A. Matzarakis, H. Rennenberg, and A. Gessler. 2006. Carbon isotopic composition and oxygen isotopic enrichment in phloem and total leaf organic matter of European beech (*Fagus sylvatica* L.) along a climate gradient. *Plant, Cell and Environment*, 29:1492–1507.
- Kenrick, P., and C. Strullu-Derrien. 2014. The origin and early evolution of roots. *Plant Physiology*, 166:570–580.
- Khalvati, M. A., Y. Hu, A. Mozafar, and U. Schmidhalter. 2005. Quantification of water uptake by arbuscular mycorrhizal hyphae and its significance for leaf growth, water relations, and gas exchange of barley subjected to drought stress. *Plant Biology*, 7:706–712.
- Krings, M., H. Kerp, T. N. Taylor, and E. L. Taylor. 2003. How Paleozoic vines and lianas got off the ground: on scrambling and climbing Carboniferous–early Permian pteridosperms. *The Botanical Review*, 69:204–224.
- Krings, M., and H. Kerp. 2006. *Neuropteris attenuata*, a narrow-stemmed, leaning or lianescent seed fern from the Upper Pennsylvanian of Lower Saxony, Germany. *Flora—Morphology, Distribution, Functional Ecology of Plants* 201:233–239.
- Krings, M., S. D. Klavins, T. N. Taylor, E. L. Taylor, R. Serbet, and H. Kerp. 2006. Frond architecture of *Odontopteris brardii* (Pteridospermopsida, ? Medullosales): new evidence from the Upper Pennsylvanian of Missouri, USA. *Journal of the Torrey Botanical Society*, 133:33–45.
- Kuromori, T., E. Sugimoto, and K. Shinozaki. 2014. Intertissue signal transfer of abscisic acid from vascular cells to guard cells. *Plant Physiology*, 164:1587–1592.
- Kurschner, W. M., J. Vanderburgh, H. Visscher, and D. L. Dilcher. 1996. Oak leaves as biosensors of late Neogene and early Pleistocene paleoatmospheric CO₂ concentrations. *Marine Micropaleontology*, 27:299–312.
- Lake, J. A., W. P. Quick, D. J. Beerling, and F. I. Woodward. 2001. Signals from mature to new leaves. *Nature*, 411:154.
- Lammertsma, E. I., H. J. De Boer, S. C. Dekker, D. L. Dilcher, A. F. Lotter and F. Wagner-Cremer. 2011. Global CO₂ rise leads to reduced maximum stomatal conductance in Florida vegetation. *Proceedings of the National Academy of Sciences*, 108:4035–4040.
- Lancashire, J. R., and A. R. Ennos. 2002. Modelling the hydrodynamic resistance of bordered pits. *Journal of Experimental Botany*, 53:1485–1493.
- Laveine, J.-P. 1986. The size of the frond in the genus *Alethopteris* Sternberg (Pteridospermopsida, Carboniferous). *Geobios*, 19:49–59.
- Laveine, J.-P., and A. Behlis. 2007. Frond architecture of the seed fern *Macroneuropteris scheuchzeri*, based on Pennsylvanian specimens from the Northern France coalfield. *Palaeontographica B*, 277:1–41.
- Laveine, J.-P., and F. Dufour. 2012. The bifurcate "outer-inner" semi-pinnate frond of the Permo-Pennsylvanian seed-fern *Neurodontopteris auriculata*, type species of the genus *Neurodontopteris*. *Palaeontographica B*, 289:75–137.
- Lawrence, D., and K. Vandecar. 2015. Effects of tropical deforestation on climate and agriculture. *Nature Climate Change*, 5:27–36.
- Lee, J.-E., B. R. Linter, J. D. Neelin, X. Jiang, P. Gentine, C. K. Boyce, J. B. Fisher, J. T. Perron, T. L. Kubar, J. Lee, and J. Worden. 2012. Reduction of tropical land region precipitation variability via transpiration. *Geophysical Research Letters*, 39:L19704.
- Loepfe, L., J. Martinez-Vilalta, J. Piñol, and M. Mencuccini. 2007. The relevance of xylem network structure for plant hydraulic efficiency and safety. *Journal of Theoretical Biology*, 247:788–803.
- Majoube, M. 1971. Fractionnement en oxygene-18 et en deuterium entre l'eau et sa vapeur. *Journal de Chimie Physique*, 58:1423–1436.
- Malone, S. R., H. S. Mayeux, H. B. Johnson, and H. W. Polley. 1993. Stomatal density and aperture length in four plant species grown across a subambient CO₂. *American Journal of Botany*, 80:1413–1418.
- Mapes, G. 1979. New synangium of presumed medullosan affinities [Abstract]. *Ohio Journal of Science*, 79:15.
- Mapes, G., and G. W. Rothwell. 1980. *Quaestora amplexa* gen. et sp. nov., a structurally simple medullosan stem from the Upper Mississippian of Arkansas. *American Journal of Botany*, 67:636–647.
- Masselter, T., N. P. Rowe, and T. Speck. 2007. Biomechanical reconstruction of the carboniferous seed fern *Lyginopteris oldhamia*: Implications for growth form reconstruction and habit. *International Journal of Plant Sciences*, 168:1177–1189.
- McCulloh, K. A., and J. S. Sperry. 2005. Patterns in hydraulic architecture and their implications for transport efficiency. *Tree Physiology*, 25: 257–267.

- McCully, M. E. 1999. Root xylem embolisms and refilling. Relation to water potentials of soil, roots, and leaves, and osmotic potentials of root xylem sap. *Plant Physiology*, 119: 1001–1008.
- McElwain, J. C., and W. G. Chaloner. 1995. Stomatal density and index of fossil plants track atmospheric carbon dioxide in the Palaeozoic. *Annals of Botany*, 76:389–395.
- McElwain, J. C., and W. G. Chaloner. 1996. The fossil cuticle as skeletal record of environmental change. *Palaios*, 11:376–388.
- Melcher, P. J., N. M. Holbrook, M. J. Burns, M. A. Zwieniecki, A.R. Cobb, T. J. Brodribb, B. Choat, and L. Sack. 2012. Measurements of stem xylem hydraulic conductivity in the laboratory and field. *Methods in Ecology and Evolution*, 3:685–694.
- Meyer-Berthaud, B., S. E. Scheckler, and J.-L. Bousquet. 2000. The development of *Archaeopteris*: new evolutionary characters from the structural analysis of an early Famennian trunk from southeast Morocco. *American Journal of Botany*, 87: 456–468.
- Mintz, J. S., S. G. Driese, and J. D. White. 2010. Environmental and ecological variability of middle Devonian (Givetian) forests in Appalachian Basin paleosols, New York, United States. *Palaios*, 25:85–96.
- Montañez, I., N. Tabor, D. Niemeier, W. A. DiMichele, T. Frank, C. Fielding, J. Isbell, L. Birgenheier, and M. Rygel. 2007. CO₂-forced climate and vegetation instability during Late Paleozoic deglaciation. *Science*, 315:87–92.
- Montañez, I. P., and C. J. Poulsen. 2013. The Late Paleozoic Ice Age: An evolving paradigm. *Annual Reviews of Earth and Planetary Sciences*, 41:13–33.
- Moreno-Gutierrez, C., G. C. Barbera, E. Nicolas, M. De Luis, V. M. Castillo, F. Martinez-Fernandez, and J. I. Querejeta. 2011. Leaf $\delta^{18}\text{O}$ of remaining trees is affected by thinning intensity in a semiarid pine forest. *Plant, Cell and Environment*, 34:1009–1019.
- Moreno-Gutierrez, C., T. E. Dawson, E. Nicolas, and J. Ignacio Querejeta. 2012. Isotopes reveal contrasting water use strategies among coexisting plant species in a Mediterranean ecosystem. *New Phytologist*, 196:489–496.
- Nishida, H. 1994. Morphology and the evolution of Cycadeoidales. *Journal of Plant Research*, 107:479–492.
- Noblin, X., L. Mahadevan, I. A. Coomaraswamy, D. A. Weitz, N. M. Holbrook, and M. A. Zwieniecki. 2008. Optimal vein density in artificial and real leaves. *Proceedings of the National Academy of Sciences*, 105:9140–9144.
- Nobre, P., M. Malagutti, D. Urbano, R. A. F. de Almeida, and E. Giarolla. 2009. Amazon deforestation and climate change in a coupled model simulation. *Journal of Climate*, 22:5686–5697.
- Nugent, K. A., and H. D. Matthews. 2012. Drivers of future northern latitude runoff change. *Atmosphere-Ocean*, 50:197–206.
- Opluštil, S., J. Pšenička, M. Libertín, A. R. Bashforth, Z. Šimůnek, J. Drábková, and J. Dašková. 2009. A Middle Pennsylvanian (Bolsovian) peat-forming forest preserved in situ in volcanic ash of the Whetstone Horizon in the Radnice Basin, Czech Republic. *Review of Palaeobotany and Palynology*, 155:234–274.
- Pfefferkorn, H. W., R. A. Gastaldo, W. A. DiMichele, and T. L. Phillips. 2008. Pennsylvanian tropical floras from the United States as a record of changing climate, p. 305–316. *In* C. R. Fielding, T. D. Frank, and J. L. Isbell (eds.), *Resolving the Late Paleozoic Ice Age in Time and Space*. Geological Society of America Special Publications 441. Boulder, CO.
- Pfefferkorn, H., W. H. Gillespie, D. A. Resnick, and M. H. Scheihing. 1984. Reconstruction and architecture of medullosan pteridosperms (Pennsylvanian). *The Mosasaur*, 2:1–8.
- Pfefferkorn, H. W., and M. C. Thomson. 1982. Changes in dominance patterns in Upper Carboniferous plant-fossil assemblages. *Geology*, 10:641–644.
- Phillips, T. L., R. A. Peppers, and W. A. DiMichele. 1985. Stratigraphic and interregional changes in Pennsylvanian coal-swamp vegetation: environmental inferences. *International Journal of Coal Geology*, 5:43–109.
- Pillitteri, L. J., and J. Dong. 2013. Stomatal Development in Arabidopsis. *The Arabidopsis Book*: e0162. doi: <http://dx.doi.org/10.1199/tab.0162>
- Pittermann, J., B. Choat, S. Jansen, S. A. Stuart, L. Lynn, and T. E. Dawson. 2010. The relationships between xylem safety and hydraulic efficiency in the Cupressaceae: The evolution of pit membrane form and function. *Plant Physiology*, 153:1919–1931.
- Pittermann, J., E. Limm, C. Rico, and M. A. Christman. 2011. Structure-function constraints of tracheid-based xylem: a comparison of conifers and ferns. *New Phytologist*, 192:449–461.
- Pittermann, J., J. S. Sperry, U. G. Hacke, J. K. Wheeler, and E. H. Sikkema. 2005. Torus-margo pits help conifers compete with angiosperms. *Science*, 310:1924–1924.
- Pittermann, J., J. S. Sperry, U. G. Hacke, J. K. Wheeler, and E. H. Sikkema. 2006. Inter-tracheid pitting and the hydraulic efficiency of conifer wood: the role of tracheid allometry and cavitation protection. *American Journal of Botany*, 93:1265–1273.
- Plotnick, R. E., F. Kenig, A. Scott, I. Glasspool, C. F.

- Eble, and W. J. Lang. 2009. Pennsylvanian paleokarst and cave fills from northern Illinois, USA: a window into late Carboniferous environments and landscapes. *Palaios*, 24:627–637.
- Pockman, W. T., and J. S. Sperry. 1997. Freezing-induced xylem cavitation and the northern limit of *Larrea tridentata*. *Oecologia*, 109:19–27.
- Pockman, W. T., and J. S. Sperry. 2000. Vulnerability to xylem cavitation and the distribution of Sonoran desert vegetation. *American Journal of Botany*, 87:1287–1299.
- Poulsen, C. J., D. Pollard, I. P. Montañez, and D. Rowley. 2007. Late Paleozoic tropical climate response to Gondwanan deglaciation. *Geology*, 35:771–774.
- Pryor, J. S. 1990. Delimiting species among permineralized medullosan pteridosperms—a plant bearing *Alethopteris* fronds from the upper Pennsylvanian of the Appalachian Basin. *Canadian Journal of Botany-Revue Canadienne De Botanique*, 68: 184–192.
- Raven, J. A. 2001. Selection pressures on stomatal evolution. *New Phytologist*, 153:371–386.
- Raven, J. A., and D. Edwards. 2001. Roots: evolutionary origins and biogeochemical significance. *Journal of Experimental Botany*, 52:381–401.
- Rockwell, F. E., J. K. Wheeler, and N. M. Holbrook. 2014. Cavitation and its discontents: opportunities for resolving current controversies. *Plant Physiology*, 164:1649–1660.
- Roden, J. S., and G. D. Farquhar. 2012. A controlled test of the dual-isotope approach for the interpretation of stable carbon and oxygen isotope ratio variation in tree rings. *Tree Physiology*, 32:490–503.
- Rössler, R. 2006. Two remarkable Permian petrified forests: correlation, comparison and significance, p. 39–63. In S. G. Lucas, G. Cassinis, and J. W. Schneider (eds.), 2006. *Non-Marine Permian Biostratigraphy and Biochronology*. Geological Society London Special Publications 265.
- Rothwell, G. W., and K. L. Whiteside. 1972. Structure of medullosan rooting systems. *American Journal of Botany*, 59: 663.
- Rowe, N. P., and T. Speck. 1998. Biomechanics of plant growth forms: The trouble with fossil plants. *Review of Palaeobotany and Palynology*, 102: 43–62.
- Rowe, N. P., and T. Speck. 2004. Hydraulics and mechanics of plants: novelty, innovation, and evolution p. 297–326. In A. R. Helmsley and I. Poole (eds.), *The Evolution of Plant Physiology*. Elsevier, London.
- Rowe, N., and T. Speck. 2005. Plant growth forms: an ecological and evolutionary perspective. *New Phytologist*, 166:61–72.
- Rowe, N.P., T. Speck, and J. Galtier. 1993. Biomechanical analysis of a Paleozoic gymnosperm stem. *Proceedings of the Royal Society of London Series B-Biological Sciences*, 252: 19–28.
- Sack, L., and N. M. Holbrook. 2006. Leaf hydraulics. *Annual Review of Plant Biology*, 57:361–381.
- Salati, E. 1987. The forest and the hydrological cycle, p. 273–296. In R. E. Dickinson (ed.), *The Geophysiology of Amazonia*. John Wiley, New York.
- Salleo, S., M. A. L. Gullo, D. D. Paoli, and M. Zippo. 1996. Xylem recovery from cavitation-induced embolism in young plants of *Laurus nobilis*: A possible mechanism. *New Phytologist*, 132:47–56.
- Scheenen, T. W. J., F. J. Vergeldt, A. M. Heemskerk, and H. van As. 2007. Intact plant magnetic resonance imaging to study dynamics in long-distance sap flow and flow-conducting surface area. *Plant Physiology*, 144:1157–1165.
- Schimmelmann, A., A. L. Sessions, and M. Mastalerz. 2006. Hydrogen isotopic (D/H) composition of organic matter during diagenesis and thermal maturation. *Annual Review of Earth and Planetary Sciences*, 34:501–33
- Schneidegger, Y., M. Saurer, M. Bahn, and R. Siegwolf. 2000. Linking stable oxygen and carbon isotopes with stomatal conductance and photosynthetic capacity: a conceptual model. *Oecologia*, 125:350–357.
- Scott, D. H. 1899. On the structure and affinities of fossil plants from the Palaeozoic rocks. III. On *Medullosa anglica*, a new representative of the Cycadofilices. *Philosophical Transactions of the Royal Society of London-Series B*, 191:81–126.
- Scott, D. H. 1914. On *Medullosa pusilla*. *Proceedings of the Royal Society of London-Series B*, 87:221–228.
- Secchi, F., and M. A. Zwieniecki. 2011. Sensing embolism in xylem vessels: the role of sucrose as a trigger for refilling. *Plant, Cell and Environment*, 34:514–524.
- Sellers, P. J., L. Bounoua, G. J. Collatz, D. A. Randall, D. A. Dazlich, S. O. Los, J. A. Berry, I. Fung, C. J. Tucker, C. B. Field, and T. G. Jensen. 1996. Comparison of radiative and physiological effects of doubled atmospheric CO₂ on climate. *Science*, 271:1402–1406.
- Serbet, R., T. N. Taylor, and E. L. Taylor. 2006. On a new medullosan pollen organ from the Pennsylvanian of North America. *Review of Palaeobotany and Palynology*, 142:219–227.
- Sperry, J. S. 1986. The form and function of the xylem. *Biorheology*, 23: 198–198.
- Sperry, J. S. 2000. Hydraulic constraints on plant gas exchange. *Agricultural and Forest Meteorology*, 104:13–23.
- Sperry, J. S. 2003. Evolution of water transport and

- xylem structure. *International Journal of Plant Sciences*, 164: S115–S127.
- Sperry, J. S., and U. G. Hacke. 2004. Analysis of circular bordered pit function – I. Angiosperm vessels with homogenous pit membranes. *American Journal of Botany*, 91:369–385.
- Sperry, J. S., U. G. Hacke, T. S. Feild, Y. Sano, and E. H. Sikkema. 2007. Hydraulic consequences of vessel evolution in angiosperms. *International Journal of Plant Sciences*, 168:1127–1139.
- Sperry, J. S., U. G. Hacke, R. Oren, and J. P. Comstock. 2002. Water deficits and hydraulic limits to leaf water supply. *Plant, Cell and Environment*, 25:251–263.
- Sperry, J. S., U. G. Hacke, and J. Pittermann. 2006. Size and function in conifer tracheids and angiosperm vessels. *American Journal of Botany*, 93:1490–1500.
- Sperry, J. S., U. G. Hacke, and J. K. Wheeler. 2005. Comparative analysis of end wall resistivity in xylem conduits. *Plant, Cell and Environment*, 28:456–465.
- Sperry, J. S., F. C. Meinzer, and K. A. McCulloh. 2008. Safety and efficiency conflicts in hydraulic architecture: scaling from tissues to trees. *Plant, Cell and Environment*, 31:632–645.
- Sperry, J. S., K. L. Nichols, J. E. M. Sullivan, and S. E. Eastlack. 1994. Xylem embolism in ring-porous, diffuse-porous, and coniferous trees of northern Utah and interior Alaska. *Ecology*, 75:1736–1752.
- Sperry, J. S., and M. T. Tyree. 1988. Mechanism of water stress-induced xylem embolism. *Plant Physiology*, 88:581–587.
- Steinthorsdottir, M., F. I. Woodward, F. Surlyk, and J. C. McElwain. 2012. Deep-time evidence of a link between elevated CO₂ concentrations and perturbations in the hydrological cycle via drop in plant transpiration. *Geology*, 40:815–818.
- Steidtmann, W. E. 1937. A preliminary report on the anatomy and affinities of *Medullosa noei* sp. nov. from the Pennsylvanian of Illinois. *American Journal of Botany*, 24:124–125.
- Steidtmann, W. E. 1944. The anatomy and affinities of *Medullosa noei* Steidtmann, and associated foliage, roots, and seeds. Contributions from the Museum of Paleontology University of Michigan, 6:131–166.
- Sterzel, J. T. 1918. Die Organischen reste des kulms und rotliegenden der gegend von chemnitz. *Abhandlungen der Mathematisch-physischen klasse der Königl. Sächsischen Gesellschaft der Wissenschaften*, 5:203–315.
- Stewart, W., and T. Delevoryas. 1952. Bases for determining relationships among the Medullosaceae. *American Journal of Botany*, 39:505–516.
- Stewart, W. N. 1950. A new species of *Medullosa*. *American Journal of Botany*, 37:674–674.
- Stewart, W. N., and T. Delevoryas. 1956. The medullosan pteridosperms. *Botanical Review*, 22:45–80.
- Stidd, B. M. 1981. The current status of medullosan seed ferns. *Review of Palaeobotany and Palynology*, 32:63–101.
- Stiller, V., J. S. Sperry, and R. Lafitte. 2005. Embolized conduits of rice (*Oryza sativa*, Poaceae) refill despite negative xylem pressure. *American Journal of Botany*, 92:1970–1974.
- Stull, G. W., W. A. DiMichele, H. J. Falcon-Lang, W. J. Nelson, and S. Elrick. 2012. Palaeoecology of *Macroneuropteris scheuchzeri*, and its implications for resolving the paradox of “xeromorphic” plants in Pennsylvanian wetlands. *Palaeogeography, Palaeoclimatology, Palaeoecology*, 331–332:162–176.
- Tabor, N. J., DiMichele, W. A., Montañez, I. P., and Chaney, D. S. 2013. Late Paleozoic continental warming of a cold tropical basin and floristic change in western Pangea. *International Journal of Coal Geology*, 119:177–186.
- Taiz, L., and E. Zeiger. 2002. *Plant Physiology*. Sinauer Associates, Inc., Sunderland, MA, 690 p. .
- Taylor, T. N., E. L. Taylor, and M. Krings. 2009. *Paleobotany: The Biology and Evolution of Fossil Plants*: Academic Press.
- Tyree, M. T., and F. W. Ewers. 1991. Tansley Review No. 34. The hydraulic architecture of trees and other woody plants. *New Phytologist*, 119:345–360.
- Tyree, M. T., S. Salleo, A. Nardini, M. A. Lo Gullo, and R. Mosca. 1999. Refilling of embolized vessels in young stems of laurel. Do we need a new paradigm? *Plant Physiology*, 120:11–21.
- Tyree, M. T., and J. S. Sperry. 1989. Vulnerability of xylem to cavitation and embolism. *Annual Review of Plant Physiology and Plant Molecular Biology*, 40:19–38.
- Tyree, M. T., and M. H. Zimmermann. 2002. *Xylem Structure and the Ascent of Sap*: Springer-Verlag, Berlin.
- van den Honert, T. H. 1948. Water transport in plants as a catenary process. *Discussions of the Faraday Society*, 3:146–153.
- Van Hoof, T. B., H. J. Falcon-Lang, C. Hartkopf-Froder, and H. Kerp. 2013. Conifer-dominated palynofloras in the middle Pennsylvanian strata of the De Lutte-6 borehole, The Netherlands: Implications for evolution, palaeoecology and biostratigraphy. *Review of Palaeobotany and Palynology*, 188:18–37.
- Wagner, R. H. 1968. Upper Westphalian and Stephanian species of Alethopteris from Europe, Asia Minor and North America. *Mededelingen van de Rijks Geologische Dienst Serie C*, 3-1 6:1–188.
- Wagner, F., D. L. Dilcher, and H. Visscher. 2005. Stomatal frequency responses in hardwood-swamp

- vegetation from Florida during a 60-year continuous CO₂ increase. *American Journal of Botany*, 92:690–695.
- Wang, S., and J. Schiefelbein. 2014. Regulation of cell fate determination in plants. *Frontiers in Plant Science*, 5:1–2.
- Werth, D., and R. Avissar. 2002. The local and global effects of Amazon deforestation. *Journal of Geophysical Research*, 107(D20):LBA 55-1–LBA 55-8.
- Wheeler, J. K., J. S. Sperry, U. G. Hacke, and N. Hoang. 2005. Inter-vessel pitting and cavitation in woody Rosaceae and other vesselless plants: a basis for a safety versus efficiency trade-off in xylem transport. *Plant, Cell and Environment*, 28:800–812.
- Williamson, W. C. 1887. *A Monograph on the Morphology and Histology of Stigmara ficoides*. The Palaeontographical Society, London, 62 p.
- Wilson, J. P., and W. W. Fischer. 2011. Geochemical support for a climbing habit within the Paleozoic seed fern genus *Medullosa*. *International Journal of Plant Sciences*, 172:586–598.
- Wilson, J. P. 2013. Modeling 400 million years of plant hydraulics. *The Paleontological Society Papers*, 19:175–194.
- Wilson, J. P., and W. W. Fischer. 2011. Hydraulics of *Asteroxylon mackei*, an early Devonian vascular plant, and the early evolution of water transport tissue in terrestrial plants. *Geobiology*, 9:121–130.
- Wilson, J. P., and A. H. Knoll. 2010. A physiologically explicit morphospace for tracheid-based water transport in modern and extinct seed plants. *Paleobiology*, 36:335–355.
- Wilson, J. P., A. H. Knoll, N. M. Holbrook, and C. R. Marshall. 2008. Modeling fluid flow in *Medullosa*, an anatomically unusual Carboniferous seed plant. *Paleobiology*, 34:472–493.
- Woodward, F. I. 1987. Stomatal numbers are sensitive to increases in CO₂ from pre-industrial levels. *Nature*, 327:617–618.
- Woodward, F. I. 1993. Plant-responses to past concentrations of CO₂. *Vegetation*, 104:145–155.
- Woodward, F. I., and C. K. Kelly. 1995. The influence of CO₂ concentration on stomatal density. *New Phytologist*, 131:311–327.
- Wnuk, C., and H. W. Pfefferkorn. 1984. The life habits and paleoecology of middle Pennsylvanian medullosan pteridosperms based on an in situ assemblage from the Bernice Basin (Sullivan County, Pennsylvania, USA). *Review of Palaeobotany and Palynology*, 41:329–351.
- Zimmermann, M. H. 1983. *Xylem Structure and the Ascent of Sap*: Springer-Verlag, Berlin.
- Zwieniecki, M. A. and N. M. Holbrook. 2009. Confronting Maxwell's demon: biophysics of xylem embolism repair. *Trends in Plant Science*, 14:530–534.

